

# GoSAFEOPT: Scalable Safe Exploration for Global Optimization of Dynamical Systems

Bhavya Sukhija<sup>a</sup>, Matteo Turchetta<sup>a</sup>, David Lindner<sup>a</sup>, Andreas Krause<sup>a</sup>, Sebastian Trimpe<sup>b</sup>, Dominik Baumann<sup>b,c</sup>

<sup>a</sup>*Department of Computer Science, ETH Zürich, Switzerland*

<sup>b</sup>*Institute for Data Science in Mechanical Engineering, RWTH Aachen University, Germany*

<sup>c</sup>*Department of Information Technology, Uppsala University, Sweden*

---

## Abstract

Learning optimal control policies directly on physical systems is challenging since even a single failure can lead to costly hardware damage. Most existing model-free learning methods that guarantee safety, i.e., no failures, during exploration are limited to local optima. A notable exception is the GoSAFE algorithm, which, unfortunately, cannot handle high-dimensional systems and hence cannot be applied to most real-world dynamical systems. This work proposes GoSAFEOPT as the first algorithm that can safely discover globally optimal policies for high-dimensional systems while giving safety and optimality guarantees. We demonstrate the superiority of GoSAFEOPT over competing model-free safe learning methods on a robot arm that would be prohibitive for GoSAFE.

*Keywords:* Model-free learning, Bayesian Optimization, Safe learning.

---

*Email addresses:* bhavya.sukhija@inf.ethz.ch (Bhavya Sukhija), matteo.turchetta@inf.ethz.ch (Matteo Turchetta), david.lindner@inf.ethz.ch (David Lindner), krausea@ethz.ch (Andreas Krause), trimpe@dsme.rwth-aachen.de (Sebastian Trimpe), dominik.baumann@it.uu.se (Dominik Baumann)

---

## 1. Introduction

Traditionally controlling a dynamical system consists in deriving a mathematical model and designing a policy based on it. The increasing complexity of modern technical systems makes this approach forbiddingly involved and time-consuming. Model-free reinforcement learning (RL) methods [1] are a promising alternative to this approach as they circumvent the modeling step by learning control policies directly from data. To succeed, they need to explore the system and its environment. Without a model, this can be arbitrarily risky and unsafe, and can ultimately damage the system. Since modern hardware such as robots are expensive and their repairs are time-consuming, safe exploration is crucial to apply model-free RL to real-world problems.

In this paper, we propose GOSAFEOPT, an algorithm that can search for globally optimal policies in complex systems without the need for a dynamics model while guaranteeing safe exploration with high probability.

### 1.1. Related Work

Recent advances in machine learning have motivated the usage of model-free RL algorithms for obtaining control policies [2; 3; 4; 5; 6]. However, directly applying these methods to the policy optimization problem in control comes with two major challenges: *(i)* Machine learning algorithms often require large amounts of data. In learning control, such data is often gathered by conducting experiments with physical systems, which is time-consuming and causes wear and tear to the hardware. *(ii)* Learning requires exploration, which can lead to unwarranted and unsafe behaviors.

One possibility to address (i) is to train models in simulation, where arbitrary amount of data can be easily collected and transfer the learned behavior to the real system. To realize this, many works have investigated how to close the *sim-to-real gap*, i.e., the inevitable gap between simulation and the real world [7; 8; 9; 10; 11]. While such methods can reduce the required amount of experiments, ultimately, we need to perform experiments on the real system to achieve optimal behaviors. When learning on real hardware, sample efficiency is crucial. Bayesian optimization (BO) [12] is a class of black-box global optimization algorithms, that has been used in a variety of works [13; 14; 15; 16] to optimize the controllers in a sample-efficient manner. However, they do not address challenge (ii).

Challenge (ii) has sparked significant work in the area of *safe RL*, see [17] for a recent survey. In safe RL, the goal is to optimize policies while guaranteeing safety at convergence and/or all times. For instance, [18] extends the trust region policy optimization algorithm [19] to account for safety. The authors of [20] incorporate safety guarantees during training for a series of dynamic programming [21] and RL algorithms, such as Deep Q-learning [22], through Lyapunov functions. The work in [23] learns a safety critic to predict the probability of failure given a state and action pair and imposes constraints on this probability. However, these methods suffer from the notoriously poor sample complexity of deep model-free RL, i.e., they do not address challenge (i).

Challenges (i) and (ii) can be addressed jointly by augmenting BO with constraints. In constrained BO, there are two main classes of methods. On the one hand, approaches like [24; 25; 26] find safe solutions but al-

low unsafe evaluations during training. Similarly, the work in [27] aims at learning safe policies while discouraging but not entirely preventing unsafe evaluations. Herein, we focus on approaches that can guarantee safety at all times during exploration, which is crucial when dealing with expensive hardware. SAFEOPT [28] and safe learning methods that emerged from it (e.g., [29; 30; 31]) guarantee safe exploration with high probability by exploiting properties of the constraint functions, e.g., regularity. Starting from an initial safe policy, these methods run experiments to gradually and locally expand the set of policies considered safe (safe set). Unfortunately, SAFEOPT and its existing variants are limited to exploring a safe set connected with the initial safe policy. Therefore, they could miss the global optimum in the presence of disjoint safe regions in the policy space (see Fig. 1). Disjoint safe regions appear when learning an impedance controller for a robot arm, as we show in our experiments and in many other applications [32; 13; 33]. To address this limitation [33] proposes GOSAFE, which can provably and safely discover the safe global optimum in the presence of disjoint safe regions under mild conditions. To achieve this, it learns safe backup policies for different states and uses them to preserve safety when evaluating policies outside of the safe set. To this end, it actively explores the joint space of initial states and policies, which is infeasible for all but the simplest systems with low-dimensional state spaces ([34] argues that an overall dimension, i.e., parameter and state space,  $d > 3$  is already challenging). As a result, GOSAFE can only handle relatively simple, low-dimensional systems.

In this work, we build upon [33] and, in particular, its mechanism of learning backup policies that allows for global exploration. To this end, we switch

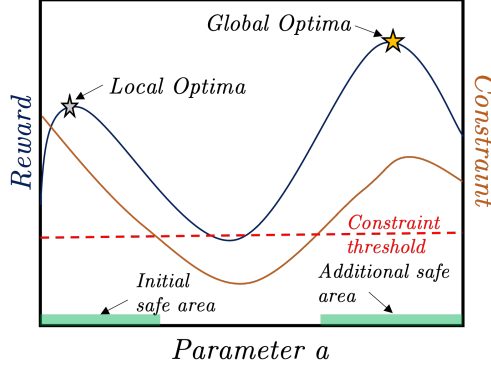


Figure 1: Illustrative example with disjoint safe regions in the policy space. The blue line depicts the objective, the orange line the constraint function, and the red dotted line the constraint threshold. The  $x$ -axis represents parameters that are used for parameterizing the policies, i.e., policy parameters. There are two safe regions that are marked in green. SAFEOPT cannot explore the global optimum if it is initialized in the left region.

between local and global steps, similar to the stagewise safe optimization algorithm proposed in [35]. However, also [35] is restricted to an optimum connected to a safe initialization while our algorithm can explore globally. The general idea of learning backup policies is related to safety filters and control barrier functions [36; 37; 38]. Nevertheless, those methods require either availability or learning of a dynamics model besides learning the policy and are, therefore, model-based. In this work, we focus on a model-free approach.

### 1.2. Contributions

This work presents GOSAFEOPT, the first model-free algorithm that can globally search for optimal policies for safety-critical, high-dimensional dynamical systems, i.e., systems with high-dimensional state spaces (systems with parameter and state space dimensions greater than three). Crucially, GOSAFEOPT leverages the *Markov property* of the system’s state to learn backup policies without actively exploring the state space and uses these



Figure 2: Franka Emika panda; seven degrees of freedom robot arm used for our evaluations.

backup policies to guarantee safety when evaluating policies outside the safe set. We provide high-probability safety guarantees for GOSAFE<sub>OPT</sub> and we prove that it recovers the safe globally optimal policy under assumptions that hold for many practical cases. Finally, we validate it in both simulated and real safety-critical path following experiments on a robotic arm (see Fig. 2), which is prohibitive for competing model-free global safe search methods. Further, we show that GOSAFE<sub>OPT</sub> achieves considerably better performance than SAFE<sub>OPT</sub>, a state-of-the-art method for model-free safe policy search for high-dimensional problems.

Table 1 compares GOSAFE<sub>OPT</sub> to the prior work on model-free safe exploration discussed in Section 1.1 in terms of safety guarantees, scalability, global exploration, and sample efficiency. It shows that GOSAFE<sub>OPT</sub> is the only model-free method that can perform sample-efficient global exploration in high-dimensional systems while providing safety guarantees.

The rest of the paper is organized as follows: after defining the problem

Table 1: Comparison between GoSAFEOPT and prior work on safe exploration based on their safety guarantees, scalability, global exploration, and sample efficiency.

	Safe exploration	High-dimensional state space	Global exploration	Sample efficient
SAFEOPT [30]	✓	✓	✗	✓
SAFEOPTSWARM [39]	✓	✓	✗	✓
SAFE LINEBO [34]	✓	✓	✗	✓
GoSAFE [33]	✓	✗	✓	✗
GoSAFEOPT (ours)	✓	✓	✓	✓

setting and introducing preliminaries in Sections 2 and 3 respectively, we present GoSAFEOPT and provide safety and optimality guarantees. Finally, in Section 5 we demonstrate in simulation and on hardware (see Fig. 2) the superiority of GoSAFEOPT over existing methods for model-free safe policy search in high-dimensional settings.

## 2. Problem Setting

We consider an unknown, Lipschitz-continuous system in differential form proposed in [33]

$$dx(t) = z(x(t), u(t)) dt, \quad (1)$$

where,  $z(\cdot)$  represents the system dynamics,  $x(t) \in \mathcal{X} \subset \mathbb{R}^s$  is the system state and  $u(t) \in \mathcal{U} \subset \mathbb{R}^p$  is the input we apply to steer the system state to follow a desired trajectory  $x_{\text{des}}(t) \in \mathcal{X}$  for all  $t \geq 0$ . We assume that the system starts at a known initial state  $x(0) = x_0$ .

The control input  $u(t)$  we apply for a given state  $x(t)$  is specified by a policy  $\pi : \mathcal{X} \times \mathcal{A} \rightarrow \mathcal{U}$ , with  $u(t) = \pi(x(t), a) := \pi^a(x(t))$ . The policy is parameterized by  $a \in \mathcal{A} \subset \mathbb{R}^d$ , where  $\mathcal{A}$  is a finite parameter space<sup>1</sup>.

<sup>1</sup>infinite parameter spaces can be handled via discretization (e.g., random subsampling)

We encode our goal of following the desired trajectory  $x_{\text{des}}(t)$  through an objective function,  $f : \mathcal{A} \rightarrow \mathbb{R}$ . Note that the objective is independent of the state space  $\mathcal{X}$ . We seek for a controller parametrization  $a \in \mathcal{A}$  that optimizes  $f$  for a constant initial condition  $x_0$ . Since the dynamics of the system in Eq. (1) are unknown, so is the objective  $f$ . Nonetheless, we assume we obtain a noisy measurement of  $f(a)$  at any  $a \in \mathcal{A}$  by running an experiment. We aim at optimizing  $f$  from these measurements in a sample-efficient way. Since deploying arbitrary policies on an unknown system can result in harmful consequences, we further formulate safety as a set of *unknown* constraints over the system trajectories that must be satisfied *at all times*. Since the trajectory of a deterministic system (1) is fully determined by its initial state and the control policy, these constraints take the form  $g_i : \mathcal{A} \times \mathcal{X} \rightarrow \mathbb{R}$  for each constraint function  $g_i$ , where  $i \in \{1, \dots, q\}$  and  $q \in \mathbb{N}$ . When considering the nominal initial condition  $x_0$ , we omit the dependency on the state  $x_0$  and write  $g_i(a)$  for simplicity. The resulting constrained optimization problem with unknown objective and constraints is:

$$\max_{a \in \mathcal{A}} f(a) \quad \text{subject to} \quad g_i(a) \geq 0, \forall i \in \{1, \dots, q\}. \quad (2)$$

In summary, *our goal is to find the optimal and safe policy parameter for the system starting with the nominal initial condition  $x_0$* . We refer to the solution of Eq. (2) as the safe global optimum  $a^*$ . Clearly, solving this problem without a dynamics model, Eq. (1), and without incurring failures for generic systems, objectives, and constraints is hopeless. The following section introduces our assumptions to make this problem tractable.



## 2.1. Assumptions

To solve the problem in Eq. (2), we must learn about the objective and the constraints without incurring failures. To start collecting data safely, we assume to have at least one initial safe policy, which could be derived from simulators or simple first principles models.

**Assumption 2.1.** A set  $S_0 \subset \mathcal{A}$  of safe parameters for the given initial condition  $x_0$  is known. That is, for all parameters  $a$  in  $S_0$  we have  $g_i(a) \geq 0$  for all  $i \in \{1, \dots, q\}$ .

In practice, similar policies often lead to similar outcomes. In other words, the objective and the constraints exhibit regularity properties. We capture this by assuming that both functions live in an reproducing kernel Hilbert space (RKHS) [40] and have bounded norm in that space.

**Assumption 2.2.** The objective  $f$  and the constraints  $g_i$  are functions in an RKHS associated to a kernel  $k$ , have bounded norms in that RKHS  $\|f\|_k \leq B$  and  $\|g_i\|_k \leq B$ , and are Lipschitz continuous with known constants.

Crucially, this assumption will allow us to infer the safety of a policy before evaluating it. While  $f$  and  $\{g_i\}_{i \in \mathcal{I}_g}$  are unknown, we assume we receive noisy measurements of them. We now formalize our assumptions on the measurement model.

**Assumption 2.3.** We obtain noisy measurements of  $f$  and  $g_i$  for all  $i \in \mathcal{I}_g$ . The measurement noise is independent and identically distributed (i.i.d)  $\sigma$ -sub-Gaussian. That is, for a measurement  $y_f$  of  $f$  (resp.  $y_{g_i}$  for measurements of  $g_i$ ), we have  $y_f = f(a) + \epsilon$  (resp.  $y_{g_i} = g_i(a) + \epsilon_{g_i}$ ) with  $\epsilon$  (resp.  $\epsilon_{g_i}$ )  $\sigma$ -sub-Gaussian.

Assumptions 2.1, 2.2, and 2.3 are common in the safe BO literature [29; 30; 28]. However, these approaches treat the evaluation of a policy as a black box. In contrast, we monitor the rollout of a policy to intervene and bring the system back to safety, if necessary. For our interventions to be effective, we assume the future trajectory of the system to depend only on its current state and not the past ones, i.e., we assume a Markovian system [41]. This is a typical assumption in RL [1] and is fulfilled for our system in Eq. (1) (see Proposition A.3 in the appendix). Furthermore, we also assume that a state measurement is received after every  $\Delta t$  seconds and that the continuous time system is well behaved in the time interval  $[t, t + \Delta t]$  for all  $t > 0$ .

**Assumption 2.4.** The state  $x(t)$  is measured after every  $\Delta t$  seconds. Furthermore, for any  $x(t)$  and  $\rho \in [0, 1]$ , the distance to  $x(t + \rho\Delta t)$  induced by any action is bounded by a known constant  $\Xi$ , that is,  $\|x(t + \rho\Delta t) - x(t)\| \leq \Xi$ .

For many real-world systems, the sampling frequencies are high compared to their time constants, and a conservative yet practical value for  $\Xi$  can be obtained from domain knowledge.

Unfortunately, a Markovian system is not sufficient to guarantee the safety of the whole trajectory. Consider the case where safety is expressed as a constraint on a cost accumulated along the trajectory. Even if we are individually safe before and after triggering a backup policy, we might be unsafe overall. Therefore, we limit the types of constraints we consider.

**Assumption 2.5.** We assume that, for all  $i \in \{1, \dots, q\}$   $g_i$  is defined as the infimum of a state-dependent function  $\bar{g}_i$  along the trajectory starting in  $x_0$

with controller  $\pi^a$ . Formally:

$$g_i(a) = \min_{x' \in \xi_{(0, x_0, a)}} \bar{g}_i(x'), \quad (3)$$

with  $\xi_{(0, x_0, a)} := \{x_0 + \int_0^t z(x(\tau); \pi^a(x(\tau))) d\tau\}$  the trajectory of  $x(t)$  under policy parameter  $a$  starting from  $x_0$  at time 0.

An example of such a constraint is the minimum distance of the system to an obstacle. Given Assumption 2.5, we can now provide a formal safety definition.

**Definition 2.6.** An experiment is safe if, for all  $t \geq 0$  and all  $i \in \{1, \dots, q\}$ ,

$$\bar{g}_i(x(t)) \geq 0. \quad (4)$$

This is a more general of defining safety for the optimization problem from Eq. (2). In particular, where Eq. (2) only considers trajectories associated to a fixed policy parameter  $a$ , Definition 2.6 also covers the case in which different portions of the trajectory are induced by different controllers.

### 3. Preliminaries

This section reviews Gaussian processes (GPs) and how to use them to construct frequentist confidence intervals, as well as relevant prior work on safe exploration (SAFEOPT and GOSAFE).

### 3.1. Gaussian Processes

To predict the objective and safety of a policy before deploying it, we want to build a model of  $f(a)$  and  $g_i(a)$ . To this end, we model our objective and constraint functions using Gaussian process regression (GPR) [42], which uses the Bayes rule to combine our prior belief and the data we collect. In GPR, our prior belief is captured by a GP, which is fully determined by a prior mean function<sup>2</sup> and a covariance function  $k(a, a')$ . Importantly, if the observations are corrupted by i.i.d Gaussian noise with variance  $\sigma^2$ , i.e.,  $y_i = f(a_i) + v_i$ , and  $v_i \sim \mathcal{N}(0, \sigma^2)$ , the posterior over  $f$  is also a GP whose mean and variance can be computed in closed form. Let us denote with  $Y_n \in \mathbb{R}^n$  the array containing  $n$  noisy observations of  $f$ , then the posterior of  $f$  at  $\bar{a}$  is  $f(\bar{a}) \sim \mathcal{N}(\mu_n(\bar{a}), \sigma_n^2(\bar{a}))$  where

$$\mu_n(\bar{a}) = k_n(\bar{a}) (K_n + I_n \sigma^2)^{-1} Y_n, \quad (5a)$$

$$\sigma_n^2(\bar{a}) = k(\bar{a}, \bar{a}) - k_n(\bar{a}) (K_n + I_n \sigma^2)^{-1} k_n^T(\bar{a}). \quad (5b)$$

The entry  $(i, j) \in \{1, \dots, n\} \times \{1, \dots, n\}$  of the covariance matrix  $K_n \in \mathbb{R}^{n \times n}$  is  $k(a_i, a_j)$ ,  $k_n(\bar{a}) = [k(\bar{a}, a_1), \dots, k(\bar{a}, a_n)]$  captures the covariance between  $x^*$  and the data, and  $I_n$  is the  $n \times n$  identity matrix.

Eq. (5) considers the case where  $f$  is a scalar function. However, we aim to model the objective  $f$  and constraints  $g_i$  with GPR. To achieve this, we use a scalar-valued function in a higher dimensional domain, proposed by [30],

---

<sup>2</sup>Assumed to be zero without loss of generality (w.l.o.g).

which describes both the objective and the constraint functions:

$$h(a, i) = \begin{cases} f(a) & \text{if } i = 0, \\ g_i(a) & \text{if } i \in \mathcal{I}_g, \end{cases} \quad (6)$$

with  $\mathcal{I}_g = \{1, \dots, q\}$ ,  $\mathcal{I} := \{0, 1, \dots, q\}$ , and  $i \in \mathcal{I}$ .

### 3.2. Frequentist Confidence Intervals

To avoid failures, we must determine the safety of a given policy before evaluating it. To this end, we reason about plausible worst-case values of the constraint  $g_i$  for a new policy  $a$ . We use the posterior distribution over constraints given by Eq. (5) to build frequentist confidence intervals, i.e., intervals where function values lie with high probability given the data. For functions fulfilling Assumption 2.2 and 2.3, [43; 44] use the GP posterior to construct frequentist confidence intervals which depend on the maximum information gain  $\gamma_n$  (cf., [45]),

$$\gamma_n := \max_{A \subset D: |A|=n} I(y_A; f_A),$$

where  $I(y_A; f_A)$  is the mutual information between  $f_A$  evaluated at points in  $A$  and the observations  $y_A$ , i.e., the amount of information  $y_A$  contains about  $f$  (see [45] for more details). For many practical kernels, like the one we consider in this work, the maximum information gain grows slowly (sublinearly) with  $n$  [43].

**Theorem 3.1.** [44, Thm.2] Let  $f$  fulfill Assumptions 2.2 and 2.3. Let  $\gamma_{n-1}$  be the maximum information gain of kernel  $k$  after  $n - 1$  iterations and

$\beta_n^{1/2} = B + \sigma\sqrt{2(\gamma_{n-1} + 1 + \ln(1/\delta))}$ . Then, for all  $a \in \mathcal{A}$  and iterations  $n \geq 1$  jointly with probability at least  $1 - \delta$ :

$$|\mu_{n-1}(a) - f(a)| \leq \beta_n^{1/2} \sigma_{n-1}(a). \quad (7)$$

### 3.3. Bayesian Optimization for Model-Free Safe Exploration

The frequentist confidence intervals presented in Section 3.2 are leveraged in SAFEOPT and GOSAFE to solve black-box constrained optimization problems, while guaranteeing safety for all the iterates with high probability. SAFEOPT guarantees safety by limiting its evaluations to a set of provably safe inputs. This safe set relies on frequentist monotonic confidence intervals based on Theorem 3.1. In particular, SAFEOPT defines the lower bound of the confidence interval  $l_n$  as  $l_n(a, i) = \max\{l_{n-1}(a, i), \mu_{n-1}(a, i) - \beta_n^{1/2} \sigma_{n-1}(a, i)\}$ , with  $l_0(a, i) = 0$  for all  $a \in S_0, i \in \mathcal{I}_g$  and  $-\infty$  otherwise, and the upper bound  $u_n$  as  $u_n(a, i) = \min\{u_{n-1}(a, i), \mu_{n-1}(a, i) + \beta_n^{1/2} \sigma_{n-1}(a, i)\}$  with  $u_0(a, i) = \infty$  for all  $a \in \mathcal{A}, i \in \mathcal{I}$ . Given a set of safe parameters  $S_{n-1}$ , it then infers the safety of nearby parameters by combining the confidence intervals with the Lipschitz continuity of the constraints:

$$S_n := \bigcap_{i \in \mathcal{I}_g} \bigcup_{a' \in S_{n-1}} \{a \in \mathcal{A} \mid l_n(a', i) - L_a \|a - a'\| \geq 0\}, \quad (8)$$

with  $L_a$  the joint Lipschitz constant of  $f(a)$ ,  $g_i(a)$ . SAFEOPT explores the safe set by evaluating points that could optimistically expand it, known as expanders  $\mathcal{G}_n$  (see Definition C.1 in Appendix C). By also evaluating potential maximizers  $\mathcal{M}_n$  (see Definition C.2 in Appendix C), it guarantees convergence to an approximately optimal solution within the largest safe reach-

able set,  $\bar{R}_\epsilon^c(S_0)$  for many practical kernels (see Eq. (A.13) in Appendix A.2 or [30; 33]). Due to the local expansion of the safe set (see Eq. (8)),  $\bar{R}_\epsilon^c(S_0)$  belongs to the safe area connected to the safe initialization. Thus, in the case of disconnected safe regions, the optimum discovered by SAFEOPT may be local (see Fig. 1).

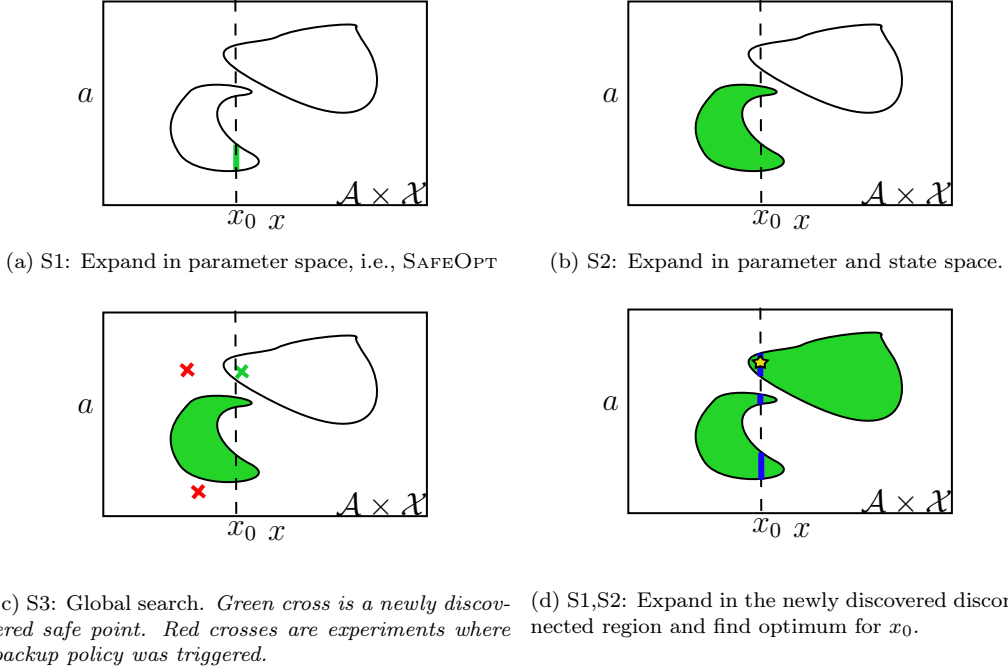


Figure 3: Illustration of GoSAFE steps. *The polygons show the safe set. The green region is the current estimate of the safe set and the golden star the optimum found by GoSAFE.*

GoSAFE [33] is an extension of SAFEOPT, which can discover disconnected safe sets while retaining high probability safety guarantees. It finds disconnected safe sets by performing a global search, i.e., evaluating potentially unsafe parameters that are not in  $S_n$ . To preserve safety during global search, GoSAFE first performs the local search of SAFEOPT in the joint parameter and state space. That is, it defines  $S_n$  as a subset of  $\mathcal{A} \times \mathcal{X}_\mu$ , where  $\mathcal{X}_\mu$

is a discretization of the continuous state space  $\mathcal{X}$  (see Definitions C.3 and C.4 in Appendix C). More concretely, GoSAFE performs safe experiments starting from initial conditions  $\tilde{x}(0)$  that are different from  $x_0$ . During global search, whenever the state  $\tilde{x}(0)$  is visited again, GoSAFE can switch to a backup policy, i.e., the policy parametrization that was safely explored in the experiment that started from  $\tilde{x}(0)$ . Thus, it can perform experiments with parameters that are potentially unsafe, monitor the system state, and trigger a backup policy if the system is about to leave the part of the state space for which it has backup policies available. The whole process is depicted in Fig. 3.

Despite its successes with low-dimensional dynamical systems, GoSAFE presents several shortcomings that hinder its scalability and therefore make its application to high-dimensional, real-world settings impossible. Particularly, learning backup policies amounts to one experiment per policy parameter and initial state. Thus, the number of experiments grows exponentially in the dimension of the domain [30; 33], which is only sustainable for simple and low-dimensional systems. Further, the discretization of the state space raises memory and computational concerns in higher dimensions. Additionally, it assumes that the system can be reset at an arbitrary safe initial condition, which is challenging even under appropriate *controllability* assumptions [46] because the system dynamics model is not known. Lastly, the boundary condition, which is needed to detect when to trigger a backup policy, proposed in [33] is costly and assumes continuous time state measurements.



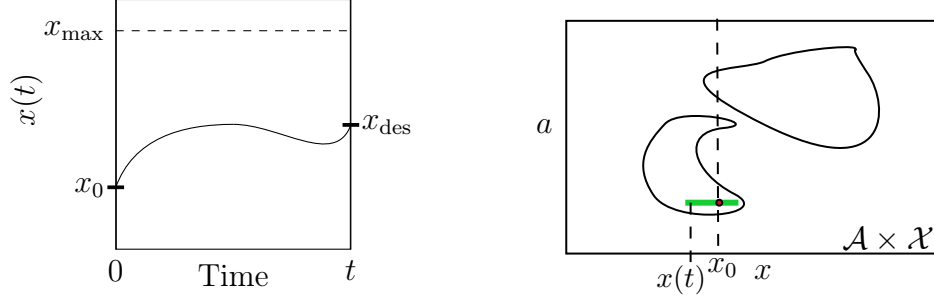
## 4. GoSAFEOPT

In this section, we present our algorithm, GoSAFEOPT, which combines the sample efficiency of SAFEOPt and the global exploration of GoSAFE to safely discover globally optimal policies for dynamical systems. To the best of our knowledge, GoSAFEOPT is the first model-free algorithm that can globally search for optimal policies, guarantee safety during exploration, and is applicable to complex hardware systems. We describe GoSAFEOPT in detail in Section 4.1 and give its safety and optimality guarantees in Section 4.3.

### 4.1. The algorithm

GoSAFEOPT consists of two alternating stages, local safe exploration (**LSE**) and global exploration (**GE**). In **LSE**, we explore the safe portion of the parameter space connected to our current estimate of the safe set. Crucially, we exploit the Markov property to learn backup policies for each state we visit during **LSE** experiments. During **GE**, we evaluate potentially unsafe policies in the hope of identifying new, disconnected safe regions. The safety of this step is guaranteed by triggering the backup policies learned during **LSE** whenever necessary. If a new disconnected safe region is identified, we switch to a **LSE** step. Otherwise, GoSAFEOPT terminates and recommends the optimum  $a^* = \arg \max_{a \in S_n} l_n(a, 0)$ .

In the following, we explain the **LSE** and **GE** stages in more detail and provide their pseudocode in Algorithms 1 and 2, respectively. Algorithm 4 presents the pseudocode for the full GoSAFEOPT algorithm.



(a) Evolution of the state  $x(t)$  under a safe policy. Here  $x_{\max}$  is defined as  $\bar{g}(x_{\max}) = 0$ .

(b) Safe set learned after the experiment. Since all the states visited during the experiment are safe, we can expand the safe set horizontally. This is in contrast to GoSAFE's **S1** where safety of only the initial state  $x_0$  is inferred.

Figure 4: Illustration of the safe set (in green) learned when utilizing the Markov property.

#### 4.1.1. Local safe exploration

Similar to SAFE<sub>OPT</sub>, during **LSE** we restrict our evaluations to provably safe policies, i.e., policies in the safe set, which is initialized with the safe seed from Assumption 2.1 and is updated recursively according to Eq. (8) (line 4 in Algorithm 1). We focus our evaluations on two relevant subsets of the safe set introduced in [28]: the maximizers  $\mathcal{M}_n$ , i.e., parameters that are plausibly optimal, and the expanders  $\mathcal{G}_n$ , i.e., parameters that, if evaluated, could optimistically enlarge the safe set. For their formal definitions, see [28] or Appendix C. During **LSE**, we evaluate the most uncertain parameter, i.e., parameter with the widest confidence interval, among the expanders and the maximizers:

$$a_n = \arg \max_{a \in \mathcal{G}_n \cup \mathcal{M}_n} \max_{i \in \mathcal{I}} w_n(a, i), \quad (9)$$

where  $w_n(a, i) = u_n(a, i) - l_n(a, i)$ .

As a by-product of these experiments, GoSAFE<sub>OPT</sub> learns backup poli-

cies for all the states visited during these rollouts by leveraging the Markov property. Intuitively, for any state  $x(t)$  visited when deploying a safe policy  $a$  starting from  $x_0$ , we know that the sub-trajectory  $\{x(\tau)\}_{\tau \geq t}$  is also safe because of Assumption 2.5. Moreover, this sub-trajectory is safe regardless of how we reach  $x(t)$  since the state is Markovian. Thus,  $a$  is a valid backup policy for  $x(t)$ .

This means we *learn about backup policies for multiple states during a single **LSE** experiment* (cf. Fig. 4). To make them available during **GE**, we introduce the set of backups  $\mathcal{B}_n \subseteq \mathcal{A} \times \mathcal{X}$ . After running an experiment with policy  $a$ , we collect all the discrete state measurements in the rollout  $\mathcal{R} = \bigcup_{k \in \mathbb{N}} \{a, x(k)\}$  and add it to the set of backups,  $\mathcal{B}_{n+1} = \mathcal{B}_n \cup \mathcal{R}$  (see Algorithm 1 line 3).

We perform **LSE** until the connected safe set is fully explored. Intuitively, this happens when we have learned our constraint functions with high precision, i.e., when the uncertainty among the expanders and maximizers is less than  $\epsilon$ , and yet the safe set does not expand any further,

$$\max_{a \in \mathcal{G}_{n-1} \cup \mathcal{M}_{n-1}} \max_{i \in \mathcal{I}} w_{n-1}(a, i) < \epsilon \text{ and } S_{n-1} = S_n, \quad (10)$$

#### 4.1.2. Global exploration

**GE** aims at discovering new, disconnected safe regions. In particular, during a **GE** step, we evaluate the most uncertain parameter outside of the safe set,  $a \in \mathcal{A} \setminus S_n$  on our system starting at the nominal initial condition  $x_0$ . As this parameter is not in our safe set, it is not guaranteed to be safe. Therefore, we monitor the state evolution during the experiment and trigger

---

**Algorithm 1** Local safe exploration (**LSE**)

---

**Input:** Safe set  $S$ , set of backups  $\mathcal{B}$ , dataset  $\mathcal{D}$

- 1: Recommend parameter  $a_n$  with Eq. (9)
- 2: Collect  $\mathcal{R} = \bigcup_{k \in \mathbb{N}} \{a_n, x(k)\}$  and  $h(a_n, i) + \varepsilon_n$
- 3:  $\mathcal{B} = \mathcal{B} \cup \mathcal{R}$ ,  $\mathcal{D} = \mathcal{D} \cup \{a_n, h(a_n, i) + \varepsilon_n\}$
- 4: Update sets  $S$ ,  $\mathcal{G}$ , and  $\mathcal{M}$  //Eq. (8), Appendix C Definitions C.1 and C.2

**Return:**  $S, \mathcal{B}, \mathcal{D}$

---

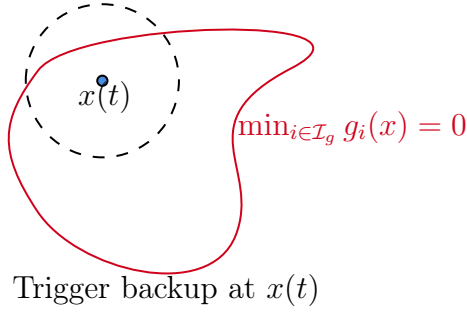


Figure 5: Illustration of the boundary condition. *The backup policy is triggered at  $x(t)$  if we cannot guarantee with high probability that all states in a ball around  $x(t)$  are safe (see Assumption 2.4 and Section 4.1.2).*

a backup policy, learned during **LSE**, if we cannot guarantee staying in a safe region of the state space when continuing with the current choice of policy parameters (cf. Fig. 5).

If a backup policy is triggered when evaluating the parameter  $a$ , we mark the experiment as failed. To avoid repeating the same experiment, we store  $a$  and the state  $x_{\text{Fail}}$  where we intervened in sets  $\mathcal{E} \subset \mathcal{A}$  and  $\mathcal{X}_{\text{Fail}} \subset \mathcal{X}$ , respectively (see line 9 in Algorithm 2). Thus, during **GE**, we employ the acquisition function

$$a_n = \arg \max_{a \in \mathcal{A} \setminus (S_n \cup \mathcal{E})} \max_{i \in \mathcal{I}_g} w_n(a, i), \quad (11)$$

which picks the most uncertain parameter, i.e., parameter with the widest confidence interval, that is not provably safe but that has not been shown to trigger a backup policy. If the experiment was run without triggering a backup, we know that  $a$  is safe. Therefore, we add the observed values for  $g_i$  and  $f$  to the dataset and the rollout  $\mathcal{R}$  collected during the experiment to our set of backups  $\mathcal{B}_n$ , i.e.,  $\mathcal{B}_{n+1} = \mathcal{B}_n \cup \mathcal{R}$ . Furthermore, we add the parameter  $a$  to our safe set, and update its lower bound, i.e.,  $l_n(a, i) = 0, \forall i \in \mathcal{I}_g$  (see lines 12 and 13 in Algorithm 2). Then, we switch to **LSE** to explore the newly discovered safe area. Note, the lower bound is updated again before the **LSE** step, i.e.,  $l_{n+1}(a, i) = \max\{l_n(a, i), \mu_n(a, i) - \beta_{n+1}^{1/2} \sigma_n(a, i)\}$  for all  $i \in \mathcal{I}_g$  (see Algorithm 4 line 6).

If  $\mathcal{A} \setminus (S_n \cup \mathcal{E}) = \emptyset$ , there are no further safe areas we can discover and **GE** has converged.

*Boundary Condition.* Throughout each **GE** experiment, we monitor the state evolution and evaluate *online* a boundary condition whenever a state measurement is received. This determines whether a backup policy should be triggered. Ideally, it must (i) guarantee safety, (ii) be fast to evaluate even for high-dimensional dynamical systems, and (iii) incorporate discrete time measurements of the state. To address (iii) Assumption 2.4 is made.

The boundary condition leverages Lipschitz continuity of the constraint to guarantee safety with high probability during **GE**, i.e., to fulfill requirement (i). In particular, when we are in  $x(t)$ , we check if there is a point  $(a_s, x_s)$  in our set of backups  $\mathcal{B}_n$  such that  $x_s$  is sufficiently close to  $x(t)$  to guarantee that  $a_s$  can steer the system back to safety for any state we may reach in the next time step.

---

**Algorithm 2** Global exploration (**GE**)

---

**Input:** Safe set  $S$ , confidence intervals  $C$ , set of backups  $\mathcal{B}$ ,

dataset  $\mathcal{D}$ , fail sets:  $\mathcal{E}$ ,  $\mathcal{X}_{\text{Fail}}$

- 1: Recommend global parameter  $a_n$  with Eq. (11)
- 2:  $a = a_n$ ,  $x_{\text{Fail}} = \emptyset$ , Boundary = False
- 3: **while** Experiment not finished **do** //Rollout policy
- 4:    $x(k) = x_0 + \int_{t=0}^{kT} z(x(t), \pi(x(t); a)) dt$
- 5:   **if** Not Boundary **then** //Not at boundary yet
- 6:     Boundary,  $a_s^* = \text{Boundary Condition}(x(t), \mathcal{B})$
- 7:     **if** Boundary **then** //Trigger backup policy
- 8:        $a = a_s^*$ ,  $x_{\text{Fail}} = x(k)$
- 9:        $\mathcal{E} = \mathcal{E} \cup \{a_n\}$ ,  $\mathcal{X}_{\text{Fail}} = \mathcal{X}_{\text{Fail}} \cup \{x_{\text{Fail}}\}$  //update fail sets
- 10: Collect  $\mathcal{R} = \bigcup_{k \in \mathbb{N}} \{a_n, x(k)\}$ , and  $h(a_n, i) + \varepsilon_n$
- 11: **if** Not Boundary **then** //Successful global search
- 12:    $\mathcal{B} = \mathcal{B} \cup \mathcal{R}$  and  $\mathcal{D} = \mathcal{D} \cup \{a_n, h(a_n, i) + \varepsilon_n\}$
- 13:    $S = S \cup a$ ,  $C(a, i) = C(a, i) \cap [0, \infty]$  for all  $i \in \mathcal{I}_g$ .

**Return:**  $S$ ,  $C$ ,  $\mathcal{B}$ ,  $\mathcal{D}$ ,  $\mathcal{E}$ ,  $\mathcal{X}_{\text{Fail}}$

---

**Boundary Condition:** During iteration  $n$ , we trigger a backup policy at  $x$  if there is no point in our set of backups  $(a_s, x_s) \in \mathcal{B}_n$  such that  $l_n(a_s, i) \geq L_x(\|x - x_s\| + \Xi)$  for all  $i \in \mathcal{I}_g$ . In this case, we use the backup parameter  $a_s^*$  with the highest safety margin, that is

$$a_s^* = \max_{\{a_s \in \mathcal{A} \mid \exists x_s \in \mathcal{X}; (a_s, x_s) \in \mathcal{B}_n\}} \min_{i \in \mathcal{I}_g} l_n(a_s, i) - L_x \|x - x_s\|. \quad (12)$$

Since we already calculate  $l_n(a_s, i)$  for all  $i \in \mathcal{I}_g$  and  $a_s \in S_n$  *offline* to update the safe set (see Eq. (8)), we only need to evaluate  $\|x - x_s\|$  *online*, which is computationally cheap. Thereby, it satisfies requirement (ii) and

---

**Algorithm 3 Boundary Condition** (Evaluation of the Boundary Condition)

---

**Input:**  $x, \mathcal{B}_n$

- 1: **if**  $\forall (a_s, x_s) \in \mathcal{B}_n, \exists i \in \mathcal{I}_g, l_n(a_s, i) - L_x(\|x - x_s\| + \Xi) < 0$  **then**
- 2:   Boundary = True, Calculate  $a_s^*$  (Eq. (12))
- 3: **else**
- 4:   Boundary = False,  $a_s^* = \{\}$

**return:** Boundary,  $a_s^*$

---

enables the application of our algorithm to complex systems with high sampling frequencies. The boundary condition is summarized in Algorithm 3.

*Updating Fail Sets.* Parameters for which the boundary condition is triggered, i.e., parameters evaluated unsuccessfully during **GE**, are added to the fail set  $\mathcal{E}$ . However, when **LSE** is repeated after discovering a new region during **GE**, we can learn new backup policies, which makes the boundary condition less restrictive. Hence, it may happen that a parameter  $a$  for which a backup policy was triggered during a previous **GE** step, i.e.,  $a \in \mathcal{E}$ , we would not trigger a backup policy after **LSE** step has converged in the new safe region. Thus, after learning new backup policies during **LSE**, we re-evaluate the boundary condition for all the states where it was previously triggered, i.e., the states in  $\mathcal{X}_{\text{Fail}}$  (line 3 to 5 in Algorithm 4), and update  $\mathcal{E}$  and  $\mathcal{X}_{\text{Fail}}$  accordingly. These states may then be revisited during further **GE** steps.

#### 4.2. Summary of GoSAFEOPt

GoSAFEOPt involves two alternating stages, **LSE** and **GE**.

- **LSE** steps are similar to SAFEOPt, nonetheless, they additionally leverage the Markov property of the system to learn backup policies.

---

**Algorithm 4** GOSAFE<sub>OPT</sub>

---

**Input:** Domain  $\mathcal{A}$ ,  $k(\cdot, \cdot)$ ,  $S_0$ ,  $C_0$ ,  $\mathcal{D}_0$ ,  $\kappa$ ,  $\eta$

```
1: Initialize GP  $h(a, i)$ ,  $\mathcal{E} = \emptyset$ ,  $\mathcal{X}_{\text{Fail}} = \emptyset$ ,  $B_0 = \{(a, x_0) \mid a \in S_0\}$ 
2: while  $S_n$  expanding or  $\mathcal{A} \setminus (S_n \cup \mathcal{E}) \neq \emptyset$  do
3:   for  $x \in \mathcal{X}_{\text{Fail}}$  do                                     //reevaluate fail sets
4:     if Not Boundary Condition( $x, \mathcal{B}_n$ ) then                 //Algorithm 3
5:        $\mathcal{E} = \mathcal{E} \setminus \{a\}$ ,  $\mathcal{X}_{\text{Fail}} = \mathcal{X}_{\text{Fail}} \setminus \{x\}$  //Update fail sets
6:   Update  $C_n(a, i) := [l_n(a, i), u_n(a, i)] \forall a \in \mathcal{A}, i \in \mathcal{I}_g$  //see Section 3.3
7:   if LSE not converged (Eq. (10)) then //Perform LSE (Algorithm 1)
8:      $S_{n+1}, \mathcal{B}_{n+1}, \mathcal{D}_{n+1} = \mathbf{LSE}(S_n, \mathcal{B}_n, \mathcal{D}_n)$ 
9:   else                                                         //Perform GE (Algorithm 2)
10:     $S_{n+1}, C_{n+1}, \mathcal{B}_{n+1}, \mathcal{D}_{n+1}, \mathcal{E}, \mathcal{X}_{\text{Fail}} = \mathbf{GE}(S_n, C_n, \mathcal{B}_n, \mathcal{D}_n, \mathcal{E}, \mathcal{X}_{\text{Fail}})$ 
return:  $\arg \max_{a \in S_n} l_n(a, 0)$ 
```

---

This is different from GOSAFE, which learns backup policies by actively exploring in the state space. As a result, GOSAFE<sub>OPT</sub> is more sample efficient than GOSAFE and can be applied for higher-dimensional systems with continuous state space. However, GOSAFE explores the safe set more exhaustively and may end up with less restrictive boundary conditions than GOSAFE<sub>OPT</sub>.

- **GE** steps follow the concepts of GOSAFE’s global exploration by triggering a backup policy when necessary to guarantee safety. However, GOSAFE<sub>OPT</sub> starts all experiments with the nominal initial condition  $x_0$ , further limiting the number of experiments and, thus, increasing sample efficiency. Additionally, it uses a new boundary condition that is more practical, cheaper to evaluate, and works for discrete time measurements.



### 4.3. Theoretical Results

This section provides safety (Section 4.3.1) and optimality (Section 4.3.2) guarantees for GOSAFEOPT.

#### 4.3.1. Safety Guarantees

The main safety result for our algorithm is that GOSAFEOPT guarantees safety during all experiments.

**Theorem 4.1.** Let Assumptions 2.1 – 2.5 hold and  $\beta_n$  be defined as in Theorem 3.1. Then, GOSAFEOPT guarantees, for all  $n \geq 0$ , that experiments are safe as per Definition 2.6 with probability at least  $1 - \delta$ .

The proof of this theorem is provided in Appendix A.1. Intuitively, since GOSAFEOPT consists of two alternating search steps (see Section 4.1), we can analyze their safety separately. Concerning the safety of **LSE**, we can leverage the results in [30], which studies it extensively. Therefore, novel to our analysis is the safety of **GE**. Specifically, the boundary condition we employ depends on the set of backups we collect by leveraging the Markov property. We show that our proposed boundary condition guarantees safety with high probability. Therefore, when running experiments during **GE**, we can guarantee that if our boundary condition triggers a backup, we are safe. Furthermore, if a backup is not triggered, then the experiment was safe, i.e., we discovered a new safe parameter.

#### 4.3.2. Optimality Guarantees

Next, we analyze when GOSAFEOPT can find the safe global optimum  $a^*$ , which is the solution to Eq. (2). GOSAFEOPT discovers new safe parameters

either during **LSE** or **GE**. During **LSE**, we explore the connected safe region. For each safe region we explore, we can leverage the results from [30] to prove local optimality. Furthermore, due to **GE**, we can discover disconnected safe regions and then repeat **LSE** to explore them. To this end, we define when a parameter  $a$  can be discovered by GOSAFEOPT (either during **LSE** or during **GE**).

**Definition 4.2.** The parameter  $a \in \mathcal{A}$  is discoverable by GOSAFEOPT at iteration  $n$ , if there exists a set  $A \subseteq S_n$  such that  $a \in \bar{R}_\epsilon^c(A)$ . Here,  $\bar{R}_\epsilon^c(A)$  is the largest safe set we can safely reach from  $A$  (see Eq. (A.13) in Appendix A.2 or [30; 33]).

Next, we show that if the safe global optimum (solution of Eq. (2)) fulfills the discoverability condition above, then we can approximate it with  $\epsilon$ -precision.

**Theorem 4.3.** Let  $a^*$  be a safe global optimum. Further, let Assumptions 2.1 – 2.5 hold,  $\beta_n$  be defined as in Theorem 3.1. Assume there exists a finite integer  $\tilde{n} \geq 0$  such that  $a^*$  is discoverable at iteration  $\tilde{n}$  (see Definition 4.2). Then, there exists a finite integer  $n^* \geq \tilde{n}$  such that with probability at least  $1 - \delta$ ,

$$f(\hat{a}_n) \geq f(a^*) - \epsilon, \quad \forall n \geq n^* \quad (13)$$

with  $\hat{a}_n = \arg \max_{a \in S_n} l_n(a, 0)$ .

In practice, GOSAFEOPT tends to find better controllers than SAFEOPT, which converges after **LSE**. This is formalized in the following proposition.

**Proposition 4.4.** For SAFEOPT,  $a^*$  is discoverable at iteration  $n > 0$ , if and only if, it is discoverable at iteration  $n = 0$ .

Proposition 4.4 states that if the parameter  $a^*$  does not lie in the largest safe set reachable from  $S_0$ , SAFE<sub>OPT</sub> will not find it. However, because in GO<sub>SAFE</sub><sub>OPT</sub> we perform a global search to discover disconnected regions, we do not suffer from the same restrictions as SAFE<sub>OPT</sub>. Furthermore, in practice, near-optimal parameters and other safe policies tend to follow similar trajectories. By collecting rollouts of safe policies, GO<sub>SAFE</sub><sub>OPT</sub> learns about safety of these trajectories. This information is leveraged during **GE** steps, where no backup policies are triggered for such safe trajectories. Therefore, in many practical applications, GO<sub>SAFE</sub><sub>OPT</sub> finds the safe global optimum (see Lemma A.17 from Appendix A.2.2 for more details).

#### 4.4. *Practical Modifications*

So far, we presented a model-free algorithm for searching globally optimal policies in high-dimensional systems that provides safety and optimality guarantees. In practice, we can further improve the sample and computational efficiency by introducing minor modifications. While they hinder our theoretical analysis, they yield good results for our evaluation in Section 5. Below we discuss these modifications.

##### 4.4.1. *Fixing Iterations for Each Stage*

In Algorithm 4, we perform a global search, i.e., **GE**, after the convergence of **LSE**. Nonetheless, it may be beneficial to run **LSE** for a fixed amount of steps and then switch to **GE**, before **LSE**’s convergence. This heuristic allows for the early discovery of disconnected safe regions, which may improve sample efficiency and the quality of early solutions. Moreover, this allows to “jump” between different safe regions of the domain that, even though

would be connected if we ran the current **LSE** to convergence, are currently disconnected. To this end, we apply the following heuristic scheme:

1. Run **LSE** for  $n_{\text{LSE}}$  steps.
2. Run **GE** for  $n_{\text{GE}}$  steps or until we have discovered new safe parameters.
3. If **GE** discovers a new region, return to 1. Else, return to 1. But with reduced  $n_{\text{LSE}}$ .

#### 4.4.2. Updated Boundary Condition

If required, the boundary condition can be further modified to reduce computation time by considering only a subset of the states collected from experiments. Specifically, the interior and marginal sets defined below.

**Definition 4.5.** Consider  $\eta_l \in \mathbb{R}$  and  $\eta_u \in \mathbb{R}$  such that  $\eta_l < \eta_u$ . The interior set  $\Omega_{I,n}$  and marginal set  $\Omega_{M,n}$  are defined as

$$\begin{aligned}\Omega_{I,n} &= \{x_s \in \mathcal{X} \mid (a, x_s) \in \mathcal{B}_n : \forall i \in \mathcal{I}_g, l_n(a, i) \geq \eta_u\} \\ \Omega_{M,n} &= \{x_s \in \mathcal{X} \mid (a, x_s) \in \mathcal{B}_n : \forall i \in \mathcal{I}_g, \eta_l \leq l_n(a, i) < \eta_u\}.\end{aligned}$$

The interior set contains the points in our set of backups  $\mathcal{B}_n$  that are safe with a high tolerance  $\eta_u$ , whereas the points in the marginal set are safe with a smaller tolerance  $\eta_l$ . We use those sets to evaluate the updated boundary condition instead of the larger set of backups  $\mathcal{B}_n$  that we collect. This further reduces the online computation time.

**Updated Boundary Condition:** Consider  $d_l \in \mathbb{R}$  and  $d_u \in \mathbb{R}$  such that  $d_l < d_u$ . We trigger a backup policy at  $x$  if there is not a point  $x_s \in \Omega_{I,n}$  such

that  $\|x - x_s\| \leq d_u$  or there is not a point  $x'_s \in \Omega_{M,n}$  such that  $\|x - x'_s\| \leq d_l$ . In this case, we use the backup parameter  $a_s^*$

$$a_s^* = \max_{\{a_s \in \mathcal{A} | (a_s, x_s) \in \mathcal{B}_n\}} l_n(a_s, i); \quad \text{with } x_s = \min_{x' \in \Omega_{I,n} \cup \Omega_{M,n}} \|x - x'\|. \quad (14)$$

Intuitively, for points  $(a_s, x_s) \in \mathcal{B}_n$  that have a high lower bound (are safe with high tolerance),  $x_s \in \Omega_{I,n}$ , our current state  $x$  can be further away ( $d_u$ ) from  $x_s$  and still be safe for the parameter  $a_s$ . This follows from the Lipschitz continuity of constraint functions. However, for points  $(a'_s, x'_s) \in \mathcal{B}_n$  that have a small lower bound, that is,  $x'_s \in \Omega_{M,n}$ , we require smaller distances  $d_l$  to ensure safety. By leveraging the ideas from the proof of Theorem 4.1 (see Appendix A.1), appropriate relations between  $\eta_u, d_u$ , respectively  $\eta_l, d_l$ , can be derived to guarantee safety.

## 5. Evaluation

We evaluate GOSAFEOPt in simulated and real-world experiments on a Franka Emika Panda seven degree of freedom (DOF) robot arm<sup>3</sup> (see Fig. 2 and 6). Our results show that GOSAFEOPt can scale to high dimensional tasks and jump to disconnected safe regions while guaranteeing safety. Furthermore, they show that GOSAFEOPt is directly applicable to hardware tasks with high sampling frequencies. More details on the experimental setup such as the objective and constraint functions are provided in Appendix B. The hyperparameters to reproduce our results are listed in Appendix D.

---

<sup>3</sup>A video of our hardware experiments and link to code are available:  
[https://sukhijab.github.io/GoSafeOpt/main\\_project.html](https://sukhijab.github.io/GoSafeOpt/main_project.html)

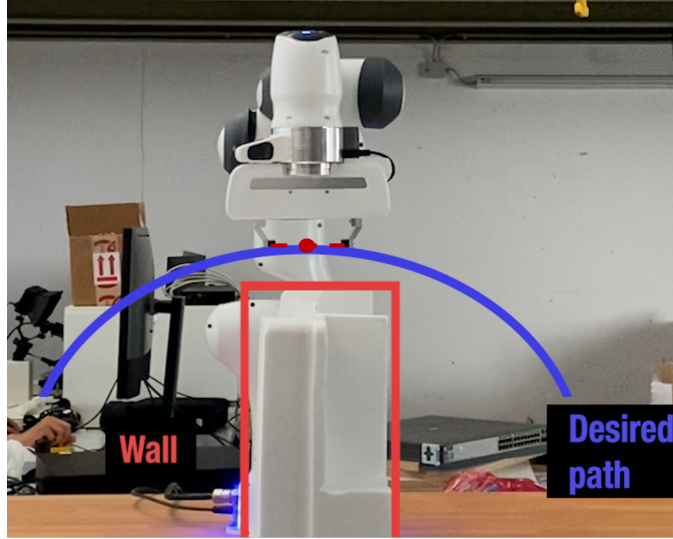


Figure 6: Setup for our evaluation in Section 5. *We consider a path following task for the Franka arm. This is a safety-critical problem since deviations from the path (blue) could cause the robot to hit the wall (red box) and incur damage.*

In all experiments with the robot arm, we solely control the position of the end-effector. To this end, we consider an operational space impedance controller [47] with impedance gain  $K$  (see Appendix B).

### 5.1. Simulation Results

We first evaluate GOSAFEOP in a simulation environment based on the Mujoco physics engine [48]<sup>4</sup>.

*Control Task:* We fix a position  $x_{\text{des}} \in \mathbb{R}^3$  which we would like the robot arm to reach. To determine the impedance gain, we use an approximate model of the system and perform feedback linearization [47]. For the resulting linear system, we design a linear-quadratic regulator (LQR) [21] with quadratic

---

<sup>4</sup>The URDFs and meshes are taken from <https://github.com/StanfordASL/PandaRobot.jl>

costs that are parameterized by matrices  $Q \in \mathbb{R}^{n \times n}$  and  $R \in \mathbb{R}^{p \times p}$ . Since the model is inaccurate, the feedback linearization will not cancel all nonlinearities and the LQR will not be optimal. Thus, our goal is to tune the cost matrices  $Q$  and  $R$  to compensate for the nonlinearities. This approach is similar to [14]. The state space we consider is six dimensional. Hence, the problem is eight-dimensional (six states, two parameters) and therefore is considered high-dimensional for safe BO. Given that the task is high dimensional, we cannot evaluate the original GOSAFE algorithm for comparison. Therefore, we compare our method to SAFEOPT.

*Optimization Problem:* We parameterize the matrices  $Q$  and  $R$  by two parameters  $(q_c, r) \in [2, 6] \times [-3, 3]$  and choose the objective function to encourage reaching the target as fast as possible while penalizing large end-effector velocities and control actions. Furthermore, we impose a constraint on the overshoot of the end-effector’s position (see Appendix B.1 for details). For analysis purposes, we run a simple grid search, that we could not run outside of simulation, to get an estimate of the safe set and the global optimum. Fig. 7 depicts the  $\epsilon$ -precise ( $\epsilon = 0.1$ ) safe set observed via grid search. From the figure, we observe that there is a disconnected safe region.

*Evaluation:* We evaluate our methods over twenty independent runs. Fig. 7 depicts the safe sets discovered by SAFEOPT and GOSAFEOPT after 200 learning iterations. We deduce from the figure that SAFEOPT is unable to discover the disconnected safe region and hence is stuck at a local optimum. On the other hand, GOSAFEOPT discovers the disconnected regions and can also jump within connected safe sets. The learning curve of the two methods is depicted in Fig. 9a. Our method performs considerably bet-

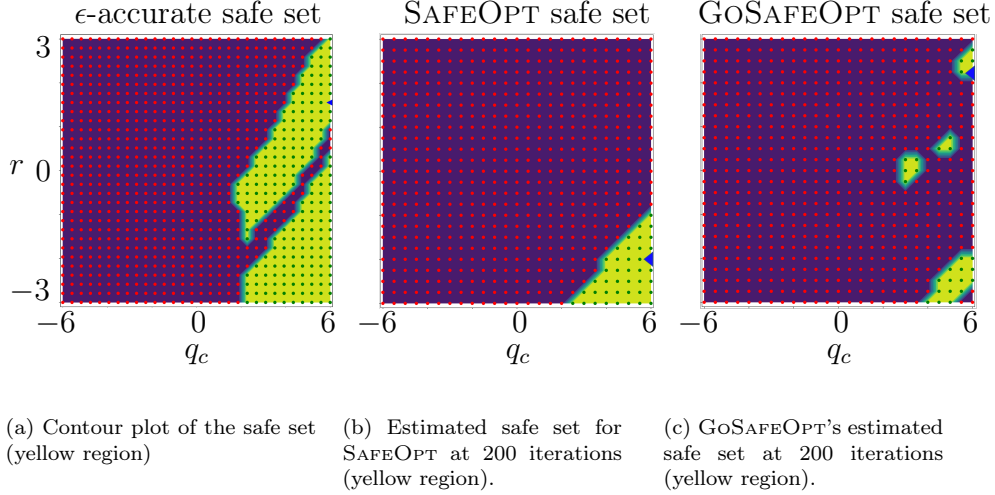


Figure 7: Comparison of the safe set for simulation task between SAFEOPT and GoSAFEOPT. *The yellow regions represent the safe sets. As can be seen, SAFEOPT discovers a connected safe set, whereas GoSAFEOPT discovers many disconnected safe islands. In each figure, the optimum is represented by a blue triangle. The optimum recommended by GoSAFEOPT lies closer to the global optimum from the true safe set, whereas SAFEOPT's recommended optimum is suboptimal.*

ter than SAFEOPT. In particular, SAFEOPT is not able to discover a better policy than the initial one after 200 iterations. This is because the initial safe seed  $S_0$  already contains a near-optimal policy from the connected region SAFEOPT explores, i.e.,  $\max_{a \in S_0} f(a) \approx \max_{a \in \bar{R}_\epsilon^c(S_0)} f(a)$ . Lastly, our method also achieves comparable safety to SAFEOPT (on average 99.9% compared to 100%). We encounter the failures during **LSE** in the second disconnected region where we suspect the constraint function has unsmooth behavior. As the failures are encountered during **LSE**, which corresponds to SAFEOPT, one could also expect similar behavior from SAFEOPT if it were initialized in the upper region.



## 5.2. Hardware Results

While the simulation results already showcased the general applicability of GoSAFE<sub>OPT</sub> to high dimensional systems and its ability to discover disconnected safe regions, we now demonstrate that it can also safely optimize policies on real world systems.

*Control Task:* We apply GoSAFE<sub>OPT</sub> to the real robot to find the optimal feedback gain matrix  $K$  for a path following task (see the experimental setup in Fig. 6). We model our controller  $K$  as

$$K = \text{diag} \left( K_x, K_y, K_z, 2\sqrt{K_x}, 2\sqrt{K_y}, 2\sqrt{K_z} \right),$$

where  $K_x = \alpha_x K_{r,x}$  with  $K_{r,x} > 0$  a reference value used for Franka’s impedance controller and  $\alpha_x \in [0, 1.2]$  the parameter we would like to tune (same for  $y, z$ ). Hence, the parameter space we consider for this task is  $[0, 1.2]^3$ .

We require the controller to follow the desired path while avoiding the wall depicted in Fig. 6. This simulates a realistic task, where the end-effector is asked to pick up an object on one side of the wall and drop it on the other.

*Optimization Problem:* We choose our objective function to encourage tracking the desired path as accurately as possible and impose a constraint on the end-effector’s distance from the wall (see Appendix B.2 for more details). We receive a measurement of the state at 250 Hz and evaluate the boundary condition during **GE** at 100 Hz.

*Evaluation:* Given the high dimension of the state space, GoSAFE cannot be applied to this task. Furthermore, the parameter space for this task is three-dimensional. Therefore, we compare our method to SAFE<sub>OPT</sub>SWARM [39], a

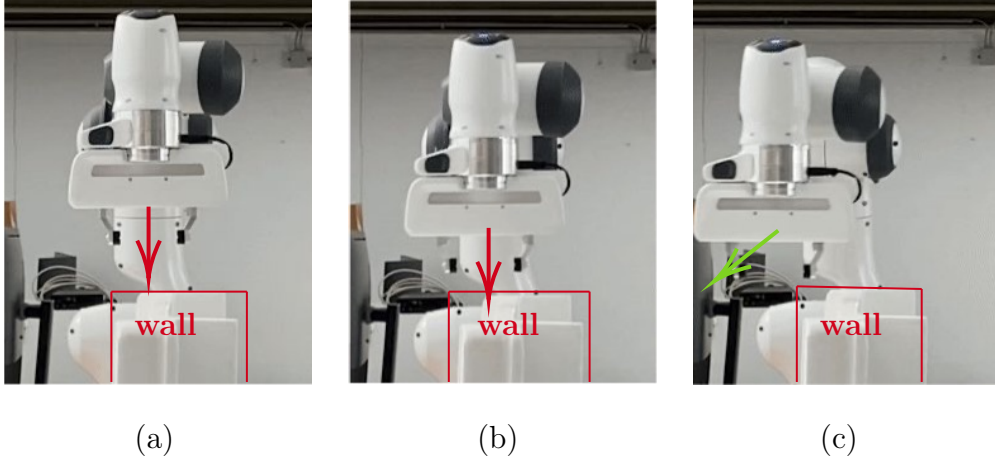


Figure 8: Illustration of triggering the backup policy during **GE**. During global search, the policy directs the robot towards the wall in (a) and (b). A backup policy is automatically triggered by our boundary condition, once the robot gets too close to the wall. The backup policy directs the robot away from the wall (see green arrow in (c)).

scalable variant of SAFE<sub>OPT</sub>, and run only 50 iterations for each algorithm in three independent runs. We attempt a global search after 20 iterations for GoSAFE<sub>OPT</sub>, perform five **GE** steps, and then revert back to **LSE**. With this, we try to find a trade-off between exploring a connected safe region (**LSE**) and discovering new safe areas with global search (**GE**).

We choose  $a_0 = (0.6, 0.6, 0.6)$  as our initial policy. During our experiments, both GoSAFE<sub>OPT</sub> and SAFE<sub>OPT</sub>SWARM provide 100% safety in all three runs. For GoSAFE<sub>OPT</sub>, safety during **GE** is preserved by triggering a backup policy if required. One such instance is shown in Fig. 8. We see in Fig. 9b that the parameters recommended by GoSAFE<sub>OPT</sub> perform considerably better than SAFE<sub>OPT</sub>SWARM. In particular, even if we cannot prove the existence of disconnected safe regions for this task, GoSAFE<sub>OPT</sub> still finds a better policy due to **GE**.

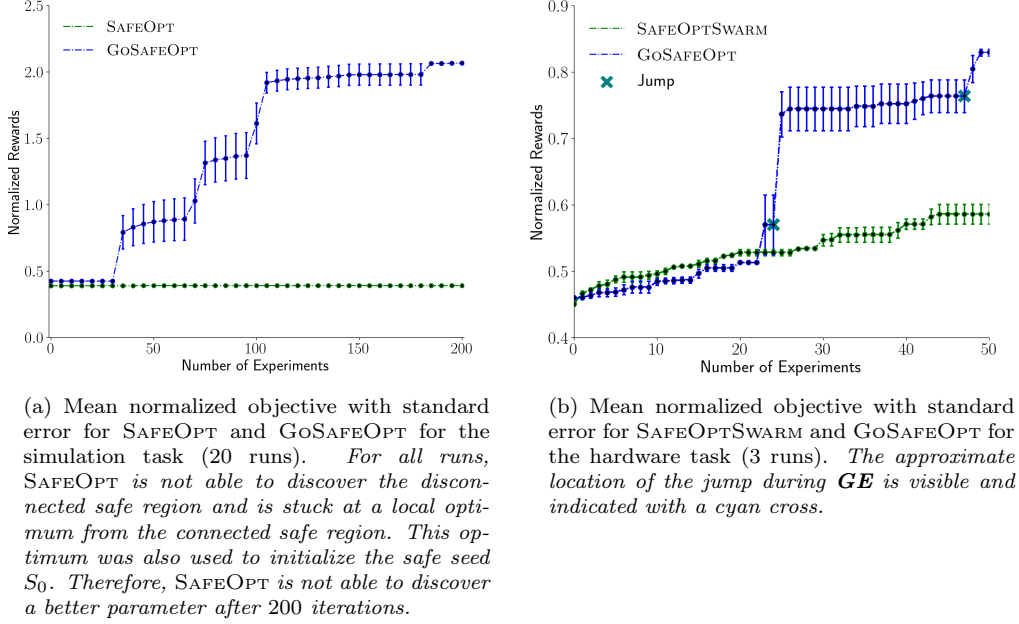


Figure 9: Objective for simulated and real world experiments.

## 6. Conclusion

This work proposes GoSAFEOPT, a novel model-free learning algorithm for global safe optimization of policies for complex dynamical systems with high-dimensional state spaces. Global safe search is enabled by learning backup policies and triggering them when the system gets too close to leaving the known safe part of the state space. We provide for GoSAFEOPT high probability safety guarantees and show that it provably performs better than SAFEOPT, a state-of-the-art model-free safe exploration algorithm for systems with high-dimensional state space. We demonstrate the superiority of our algorithm over SAFEOPT empirically through our experiments. GoSAFEOPT can handle more complex and realistic dynamical systems compared to existing model-free learning methods for safe global exploration,

such as GOSAFE. This is due to a combination of an efficient passive discovery of backup policies that leverages the Markov property of the system and a novel and efficient boundary condition to detect when to trigger a backup policy.

GOSAFE and GOSAFE<sub>OPT</sub> represent two extreme ends of a continuous spectrum: while GOSAFE exhaustively explores the state space for backup policies, GOSAFE<sub>OPT</sub> completely forgoes active exploration and leverages the Markov property instead. Clearly, one could design hybrid algorithms that leverage the Markov property *and* actively explore the state space.

## Acknowledgements

We would like to thank Kyrylo Sovailo for helping us with the hardware experiments on the Franka Emika Panda arm. Furthermore, we would also like to thank Christian Fiedler, Pierre-François Massiani, and Steve Heim for their feedback on this work.

This project has received funding from the Federal Ministry of Education and Research (BMBF) and the Ministry of Culture and Science of the German State of North Rhine-Westphalia (MKW) under the Excellence Strategy of the Federal Government and the Länder, the European Research Council (ERC) under the European Union’s Horizon 2020 research and innovation program grant agreement No 815943, the Swiss National Science Foundation under NCCR Automation, grant agreement 51NF40 180545, and the Microsoft Swiss Joint Research Center.

## References

- [1] R. S. Sutton, A. G. Barto, Reinforcement Learning: An Introduction, 2nd Edition, The MIT Press, 2018.
- [2] S. Levine, C. Finn, T. Darrell, P. Abbeel, End-to-end training of deep visuomotor policies, *The Journal of Machine Learning Research* 17 (1) (2016) 1334–1373.
- [3] J. Peters, S. Schaal, Reinforcement learning of motor skills with policy gradients, *Neural networks* 21 (4) (2008) 682–697.
- [4] T. P. Lillicrap, J. J. Hunt, A. Pritzel, N. Heess, T. Erez, Y. Tassa, D. Silver, D. Wierstra, Continuous control with deep reinforcement learning, *arXiv preprint arXiv:1509.02971* (2015).
- [5] J. Kober, J. A. Bagnell, J. Peters, Reinforcement learning in robotics: A survey, *The International Journal of Robotics Research* 32 (11) (2013) 1238–1274.
- [6] S. Schaal, C. G. Atkeson, Learning control in robotics, *IEEE Robotics & Automation Magazine* 17 (2) (2010) 20–29.
- [7] X. B. Peng, M. Andrychowicz, W. Zaremba, P. Abbeel, Sim-to-real transfer of robotic control with dynamics randomization, in: *2018 IEEE International Conference on Robotics and Automation (ICRA)*, 2018, pp. 3803–3810. doi:10.1109/ICRA.2018.8460528.
- [8] J. Hwangbo, J. Lee, A. Dosovitskiy, D. Bellicoso, V. Tsounis, V. Koltun,

- M. Hutter, Learning agile and dynamic motor skills for legged robots, *Science Robotics* 4 (26) (2019) eaau5872.
- [9] J. Lee, J. Hwangbo, L. Wellhausen, V. Koltun, M. Hutter, Learning quadrupedal locomotion over challenging terrain, *Science Robotics* 5 (47) (2020) eabc5986.
- [10] J. Siekmann, Y. Godse, A. Fern, J. Hurst, Sim-to-real learning of all common bipedal gaits via periodic reward composition, in: *IEEE International Conference on Robotics and Automation (ICRA)*, 2021, pp. 7309–7315.
- [11] J. Siekmann, K. Green, J. Warila, A. Fern, J. Hurst, Blind Bipedal Stair Traversal via Sim-to-Real Reinforcement Learning, in: *Proceedings of Robotics: Science and Systems, Virtual*, 2021. doi:10.15607/RSS.2021.XVII.061.
- [12] J. Mockus, V. Tiesis, A. Zilinskas, The application of Bayesian methods for seeking the extremum, *Towards Global Optimization* 2 (117-129) (1978) 2.
- [13] R. Calandra, A. Seyfarth, J. Peters, M. Deisenroth, Bayesian optimization for learning gaits under uncertainty, *Annals of Mathematics and Artificial Intelligence* 76 (2016) 5–23.
- [14] A. Marco, P. Hennig, J. Bohg, S. Schaal, S. Trimpe, Automatic LQR tuning based on Gaussian process global optimization, in: *IEEE International Conference on Robotics and Automation*, 2016, pp. 270–277.

- [15] R. Antonova, A. Rai, C. G. Atkeson, Deep kernels for optimizing locomotion controllers, in: Conference on Robot Learning, 2017, pp. 47–56.
- [16] M. Turchetta, A. Krause, S. Trimpe, Robust model-free reinforcement learning with multi-objective Bayesian optimization, in: IEEE International Conference on Robotics and Automation, 2020, pp. 10702–10708.
- [17] L. Brunke, M. Greeff, A. W. Hall, Z. Yuan, S. Zhou, J. Panerati, A. P. Schoellig, Safe learning in robotics: From learning-based control to safe reinforcement learning, Annual Review of Control, Robotics, and Autonomous Systems (2021).
- [18] J. Achiam, D. Held, A. Tamar, P. Abbeel, Constrained policy optimization, in: International Conference on Machine Learning, 2017, pp. 22–31.
- [19] J. Schulman, S. Levine, P. Abbeel, M. Jordan, P. Moritz, Trust region policy optimization, in: International Conference on Machine Learning, 2015, pp. 1889–1897.
- [20] Y. Chow, O. Nachum, E. Duenez-Guzman, M. Ghavamzadeh, A Lyapunov-based approach to safe reinforcement learning, in: Advances in Neural Information Processing Systems, 2018, p. 8103–8112.
- [21] D. P. Bertsekas, Dynamic Programming and Optimal Control, 2nd Edition, Athena Scientific, 2000.
- [22] V. Mnih, K. Kavukcuoglu, D. Silver, A. Graves, I. Antonoglou, D. Wierstra, M. Riedmiller, Playing Atari with deep reinforcement learning, NeurIPS Deep Learning Workshop (2013).

- [23] K. Srinivasan, B. Eysenbach, S. Ha, J. Tan, C. Finn, Learning to be safe: Deep RL with a safety critic, arXiv preprint arXiv:2010.14603 (2020).
- [24] M. Gelbart, J. Snoek, R. Adams, Bayesian optimization with unknown constraints, Conference on Uncertainty in Artificial Intelligence (2014) 250–259.
- [25] J. M. Hernández-Lobato, M. A. Gelbart, R. P. Adams, M. W. Hoffman, Z. Ghahramani, A general framework for constrained Bayesian optimization using information-based search, The Journal of Machine Learning Research 17 (1) (2016) 5549–5601.
- [26] A. Marco, D. Baumann, M. Khadiv, P. Hennig, L. Righetti, S. Trimpe, Robot learning with crash constraints, IEEE Robotics and Automation Letters 6 (2) (2021) 1439–1446.
- [27] S. Heim, A. Rohr, S. Trimpe, A. Badri-Spröwitz, A learnable safety measure, in: Conference on Robot Learning, 2020, pp. 627–639.
- [28] Y. Sui, A. Gotovos, J. Burdick, A. Krause, Safe exploration for optimization with Gaussian processes, in: International Conference on Machine Learning, 2015, pp. 997–1005.
- [29] F. Berkenkamp, A. P. Schoellig, A. Krause, Safe controller optimization for quadrotors with Gaussian processes, in: IEEE International Conference on Robotics and Automation, 2016, pp. 491–496.
- [30] F. Berkenkamp, A. Krause, A. P. Schoellig, Bayesian optimization with safety constraints: safe and automatic parameter tuning in robotics, Machine Learning (2021).



- [31] C. König, M. Turchetta, J. Lygeros, A. Rupenyan, A. Krause, Safe and efficient model-free adaptive control via Bayesian optimization, arXiv preprint arXiv:2101.07825 (2021). `arXiv:2101.07825`.
- [32] E. N. Gryazina, B. T. Polyak, Stability regions in the parameter space: D-decomposition revisited, *Automatica* 42 (1) (2006) 13–26.
- [33] D. Baumann, A. Marco, M. Turchetta, S. Trimpe, GoSafe: Globally optimal safe robot learning, in: *IEEE International Conference on Robotics and Automation*, 2021, pp. 4452–4458, Proofs in extended online version: `arXiv 2105.13281`.
- [34] J. Kirschner, M. Mutny, N. Hiller, R. Ischebeck, A. Krause, Adaptive and safe Bayesian optimization in high dimensions via one-dimensional subspaces, in: *International Conference on Machine Learning*, 2019, pp. 3429–3438.
- [35] Y. Sui, V. Zhuang, J. Burdick, Y. Yue, Stagewise safe Bayesian optimization with Gaussian processes, in: *International Conference on Machine Learning*, 2018, pp. 4781–4789.
- [36] K. P. Wabersich, M. N. Zeilinger, A predictive safety filter for learning-based control of constrained nonlinear dynamical systems, *Automatica* 129 (2021) 109597.
- [37] P. Wieland, F. Allgöwer, Constructive safety using control barrier functions, *IFAC Proceedings Volumes* 40 (12) (2007) 462–467.
- [38] R. Cheng, G. Orosz, R. M. Murray, J. W. Burdick, End-to-end safe reinforcement learning through barrier functions for safety-critical contin-

- uous control tasks, in: AAAI Conference on Artificial Intelligence, 2019, pp. 3387–3395.
- [39] R. R. Duivenvoorden, F. Berkenkamp, N. Carion, A. Krause, A. P. Schoellig, Constrained Bayesian optimization with particle swarms for safe adaptive controller tuning, IFAC-PapersOnLine 50 (1) (2017) 11800–11807, 20th IFAC World Congress.
  - [40] B. Schölkopf, A. J. Smola, Learning with Kernels: Support Vector Machines, Regularization, Optimization, and Beyond, MIT Press, Cambridge, MA, USA, 2001.
  - [41] M. L. Puterman, Markov decision processes: discrete stochastic dynamic programming, John Wiley & Sons, 2014.
  - [42] C. E. Rasmussen, C. K. I. Williams, Gaussian Processes for Machine Learning (Adaptive Computation and Machine Learning), The MIT Press, 2005.
  - [43] N. Srinivas, A. Krause, S. M. Kakade, M. W. Seeger, Information-theoretic regret bounds for Gaussian process optimization in the bandit setting, IEEE Transactions on Information Theory 58 (5) (2012) 3250–3265.
  - [44] S. R. Chowdhury, A. Gopalan, On kernelized multi-armed bandits, in: International Conference on Machine Learning, 2017, pp. 844–853.
  - [45] T. M. Cover, J. A. Thomas, Elements of Information Theory (Wiley Series in Telecommunications and Signal Processing), Wiley-Interscience, USA, 2006.

- [46] R. E. Kalman, Contributions to the theory of optimal control, Boletín de la Sociedad Matemática Mexicana 5 (2) (1960) 102–119.
- [47] B. Siciliano, O. Khatib, Springer Handbook of Robotics, 2nd Edition, Springer Publishing Company, Incorporated, 2016.
- [48] E. Todorov, T. Erez, Y. Tassa, Mujoco: A physics engine for model-based control, in: IEEE/RSJ International Conference on Intelligent Robots and Systems, 2012, pp. 5026–5033.

## A. Proofs of Theoretical Results

In this section, we provide proofs for the theoretical results stated in the main body of the paper. In the following, we denote by  $k$  discrete time indices and with  $t$  continuous ones. This difference is important because, while we obtain state measurements at discrete times, we need to preserve safety at all times. Moreover, similarly to the notation in GoSAFE [33], we denote by  $\xi_{(t,x(t),a)} = \{x(t) + \int_t^{t'} z(x(\tau); \pi^a(x(\tau)))d\tau \mid t' \geq t\}$  all the states in the trajectory induced by the policy  $a$  starting from  $x(t)$  at time  $t$ .

### A.1. Safety Guarantees

In the following, we prove Theorem 4.1, which gives the safety guarantees for GoSAFE<sub>OPT</sub>. Since GoSAFE<sub>OPT</sub> has two stages, **LSE** and **GE**, we can study their safety separately. For **LSE**, [30] provides safety guarantees. Therefore, here we focus on the safety guarantees for **GE** and then show that combining both will guarantee safety of the overall algorithm. To this end, we first make a hypothesis on our safe set  $S_n$  and confidence bounds  $l_n(a, i)$  and  $u_n(a, i)$ .

**Hypothesis A.1.** Let  $S_n \neq \emptyset$ . The following properties hold for all  $i \in \mathcal{I}_g$ ,  $n \geq 0$  with probability at least  $1 - \delta$ :

$$\forall a \in S_n : g_i(a, x_0) \geq 0, \tag{A.1}$$

$$\forall a \in \mathcal{A} : l_n(a, i) \leq g_i(a, x_0) \leq u_n(a, i). \tag{A.2}$$

We leverage this hypothesis to prove that we are safe during **GE** and then we show that it is satisfied for GoSAFE<sub>OPT</sub>. Particularly, during **LSE**,

[30] proves that our hypothesis is fulfilled. Hence, before **GE**, the safe set and the confidence intervals satisfy it. In the following, we show the updates of the safe sets and the confidence intervals implemented by **GE** also satisfy our hypothesis, which is sufficient to conclude that the hypothesis is satisfied for all  $n \geq 0$  (we will make this concrete in Lemma A.9).

During **GE**, we receive measurements of the state in discrete times and evaluate our boundary condition to trigger a backup policy if necessary. Therefore, we first show that even with discrete time measurements, we can still guarantee safety in continuous time. In particular, we start by providing conditions on the values of the constraint at those discrete times,  $g_i(a, x(k))$ , which ensure safety in continuous time, i.e.,  $\bar{g}_i(x(t)) \geq 0$  for all  $t \in [k\Delta t, (k+1)\Delta t]$ .

**Lemma A.2.** Let Assumptions 2.4 and 2.5 hold and let  $k_+ \geq k_- \geq 0$  be arbitrary integers. If, for all integers  $k \in [k_-, k_+]$ , there exists  $a_s \in \mathcal{A}$  such that  $g_i(a_s, x(k)) \geq L_x \Xi$  for all  $i \in \mathcal{I}_g$ , then  $\bar{g}_i(x(t)) \geq 0$ , for all  $t \in [k_- \Delta t, (k_+ + 1)\Delta t]$  and  $i \in \mathcal{I}_g$ .

*Proof.* By choice of the sampling scheme, we have that the state  $x(k)$  measured in discrete time, corresponds to the the state  $x(k\Delta t)$  in continuous time. Hence,  $g_i(a_s, x(k)) = g_i(a_s, x(k\Delta t))$ . Consider some  $k \geq 0$  and  $a_s \in \mathcal{A}$  such that  $g_i(a_s, x(k\Delta t)) \geq L_x \Xi$ . For any  $t \in [k\Delta t, (k+1)\Delta t]$  we have

$$\begin{aligned} g_i(a_s, x(k\Delta t)) - g_i(a_s, x(t)) &\leq L_x \|x(k\Delta t) - x(t)\| \\ &\quad \text{(Lipschitz continuity (Assumption 2.2))} \\ &\leq L_x \Xi. \quad \text{(Assumption 2.4)} \end{aligned}$$

Now, since  $g_i(a_s, x(k\Delta t)) \geq L_x \Xi$ , we have, for all  $t \in [k\Delta t, (k+1)\Delta t]$  and  $i \in \mathcal{I}_g$ ,

$$g_i(a_s, x(t)) \geq g_i(a_s, x(k\Delta t)) - L_x \Xi \geq 0. \quad (\text{A.3})$$

For our choice of constraints (Assumption 2.5) this implies  $\bar{g}_i(x(t)) \geq 0$  for all  $i \in \mathcal{I}_g$  and  $t \in [k\Delta t, (k+1)\Delta t]$ . Finally, since this holds for all integers  $k$  with  $k_- \leq k \leq k_+$ , it also holds for all  $t \in [k_- \Delta t, (k_+ + 1)\Delta t]$ .  $\square$

Now we have established a condition which guarantees for a given time interval that  $\bar{g}_i(x(t)) \geq 0$  for all  $i \in \mathcal{I}_g$ . Intuitively, the condition says that if there is a safe parameter  $a_s$  for  $x(k)$ , which gives a policy that guarantees safety with high enough tolerance, then we can guarantee safety up until the next time step  $k+1$  irrespective of what policy we apply. Hence, the tolerance  $L_x \Xi$ , takes the worst-case state evolution (according to Assumption 2.4) over a discrete time step  $\Delta t$  into account.

We collect parameter and state combinations during rollouts in our set of backups  $\mathcal{B}_n$ . The intuition here is that for a Markovian system all states visited during a safe experiment are also safe. This is important as it allows GOSAFE<sub>OPT</sub> to learn backup policies for multiple states without actively exploring the state space. We formalize this in the following proposition.

**Proposition A.3.** Let Assumption 2.5 hold. If  $(a, x_0)$  is safe, that is,  $\min_{x' \in \xi_{(0, x_0, a)}} \bar{g}_i(x') \geq 0$  for all  $i \in \mathcal{I}_g$ , then, for all  $t_1 \geq 0$ ,  $(a, x(t_1))$  is also safe, that is  $\min_{x' \in \xi_{(t_1, x(t_1), a)}} \bar{g}_i(x') \geq 0$  for all  $i \in \mathcal{I}_g$ .

*Proof.* The system in Eq. (1) is Markovian, i.e., for any  $x(t_1) \in \xi_{(0, x_0, a)}$  and

$x(t_2) \in \xi_{(0,x_0,a)}$  with  $t_2 > t_1 > 0$ ,

$$\begin{aligned} x(t_2) &= x_0 + \int_0^{t_1} z(x(t); \pi^a(x(t)))dt + \int_{t_1}^{t_2} z(x(t); \pi^a(x(t)))dt \\ &= x(t_1) + \int_{t_1}^{t_2} z(x(t); \pi^a(x(t)))dt. \end{aligned}$$

Therefore, a trajectory starting in  $x(t_1)$  will always result in the same state evolution, independent of how we arrived at  $x(t_1)$ . Combining this and Assumption 2.5, we get

$$\begin{aligned} g_i(a, x(t_1)) &= \min_{x' \in \xi_{(t_1, x(t_1), a)}} \bar{g}_i(x') && \text{Assumption 2.5} \\ &\geq \min_{x' \in \xi_{(0, x_0, a)}} \bar{g}_i(x') && \text{Markov Property} \\ &= g_i(a, x_0) && \text{Assumption 2.5} \\ &\geq 0. \end{aligned}$$

□

We have now established that our set of backups  $\mathcal{B}_n$  consists of safe parameter and state combinations. Nonetheless, in GoSAFE<sub>OPT</sub>, we do not model the constraint function for each  $(a_s, x_s) \in \mathcal{B}_n$ , i.e.,  $g_i(a_s, x_s)$ . Specifically, for our boundary condition (Section 4.1.2), we use  $l_n(a_s, i)$ , a lower bound on the function  $g_i(a_s, x_0)$ . In the following, we show that  $g_i(a_s, x_0)$  itself is a lower bound for all points  $(a_s, x_s)$  in  $\mathcal{B}_n$ , i.e.,  $g_i(a_s, x_s) \geq g_i(a_s, x_0)$ . This will play a crucial role in showing that we preserve safety whenever we trigger a backup policy.

**Corollary A.4.** Let Assumption 2.5 hold. For all points  $(a_s, x_s)$  in  $\mathcal{B}_n$ ,  $g_i(a_s, x_s) \geq g_i(a_s, x_0)$  for all  $i \in \mathcal{I}_g$ .

*Proof.* Each point  $(a_s, x_s)$  in  $\mathcal{B}_n$  is collected during a safe experiments (see Algorithm 1 line 3 and Algorithm 2 line 12). Therefore,  $x_s \in \xi_{(0, x_0, a_s)}$ . The result then follows from Proposition A.3.  $\square$

Corollary A.4 shows that  $l_n(a_s, i)$  is a conservative lower bound on  $g_i(a_s, x_s)$ . Crucially, if we can observe not just the rollouts but also the constraint values  $g_i(a_s, x_s)$ , we could model them with a GP to obtain a potentially less conservative lower bound. However, in our work we only assume that we can measure  $g_i(a_s, x_0)$  (Assumption 2.3).

Proposition A.3 and Corollary A.4 formalize how we collect our backup policies and leverage them in our boundary condition. In the following, we prove that experiments, where we trigger a backup policy, are safe. First, we show that if the boundary condition is triggered at a time step  $k^*$ , then we are safe up until  $k^* \Delta t$ , i.e., time of trigger.

**Lemma A.5.** Let the assumptions from Theorem 4.1 and Hypothesis A.1 hold. If, during **GE**, the boundary condition from Algorithm 3 triggers a backup policy at time step  $k^* > 0$ , then, for all  $t \leq k^* \Delta t$  and  $i \in \mathcal{I}_g$ ,  $\bar{g}_i(x(t)) \geq 0$  with probability at least  $1 - \delta$ .

*Proof.* Consider  $k < k^*$ . Since the boundary condition (Algorithm 3) did not trigger a backup policy at  $k$ , we have

$$\exists (a_s, x_s) \in \mathcal{B}_n \text{ such that } l_n(a_s, i) \geq L_x (\|x(k) - x_s\| + \Xi), \forall i \in \mathcal{I}_g. \quad (\text{A.4})$$



By Lipschitz continuity of  $g$ , we have

$$g_i(a_s, x_s) - g_i(a_s, x(k)) \leq L_x \|x(k) - x_s\|, \quad (\text{A.5})$$

which implies

$$\begin{aligned} g_i(a_s, x(k)) &\geq g_i(a_s, x_s) - L_x \|x(k) - x_s\| \\ &\geq g_i(a_s, x_0) - L_x \|x(k) - x_s\| && \text{Corollary A.4} \\ &\geq l_n(a_s, i) - L_x \|x(k) - x_s\| && \text{Hypothesis A.1} \\ &\geq L_x \Xi && (\text{A.4}) \end{aligned}$$

for all  $i \in \mathcal{I}_g$  and  $k < k^*$ . Therefore, we can use Lemma A.2 to prove the claim by choosing  $k_- = 0$  and  $k_+ = k^* - 1$ . □

Lemma A.5 shows that up until the time we trigger our boundary condition, we are safe with enough tolerance ( $L_x \Xi$ ) to guarantee safety. In the following, we show that if we trigger a safe backup policy at  $k^*$ , we will fulfill our constraints for all times after triggering.

**Lemma A.6.** Let the assumptions from Theorem 4.1 and Hypothesis A.1 hold. If during a **GE** experiment with parameter  $a_{\mathbf{GE}}$  at time step  $k^* \geq 0$ , our boundary condition triggers the backup policy  $a_s^*$  defined as (see Eq. (12))

$$a_s^* = \arg \max_{\{a \in \mathcal{A} \mid \exists x \in \mathcal{X}; (a, x) \in \mathcal{B}_n\}} \min_{i \in \mathcal{I}_g} l_n(a, i) - L_x \|x - x(k^*)\|. \quad (\text{A.6})$$

Then for all  $t \geq k^* \Delta t$ ,  $\bar{g}_i(x(t)) \geq 0$  for all  $i \in \mathcal{I}_g$  with probability at least

$1 - \delta$ .

*Proof.* We want to show that Eq. (A.6) finds a parameter  $a_s^*$  such that  $g_i(a_s^*, x(k^*)) \geq 0$ . For  $k^* = 0$ , this follows by definition because  $\mathcal{B}_n$  consists of safe rollouts (see Algorithm 1 line 3 and Algorithm 2 line 12) and thus, for all parameters  $a_s$  in  $\mathcal{B}_n$  and  $i \in \mathcal{I}_g$ , we have  $g_i(a_s, x_0) \geq 0$ .

Let us now consider any integer  $k^* > 0$ . Let  $(a_s, x_s) \in \mathcal{B}_n$  be arbitrary. Following the same Lipschitz continuity based arguments as in Lemma A.5, we have for all  $i \in \mathcal{I}_g$ ,

$$\begin{aligned}
g_i(a_s, x(k^*)) &\geq l_n(a_s, i) - L_x \|x_s - x(k^*)\| && \text{same as Lemma A.5} \\
&\geq l_n(a_s, i) - L_x (\|x(k^* - 1) - x_s\| + \|x(k^*) - x(k^* - 1)\|) \\
&&& \text{(Triangle inequality)} \\
&\geq l_n(a_s, i) - L_x (\|x(k^* - 1) - x_s\| + \Xi) && \text{(Assumption 2.4)} \\
&\geq 0, && \text{(A.7)}
\end{aligned}$$

where the last inequality follows from the fact that the boundary condition was not triggered at time step  $k^* - 1$  (see Section 4.1.2). Furthermore, from Eq. (A.7) we can conclude that there exists  $a_s \in \mathcal{A}$  such that for some  $x_s \in \mathcal{X}$ ,  $(a_s, x_s) \in \mathcal{B}_n$ , and  $l_n(a_s, i) - L_x \|x_s - x(k^*)\| \geq 0$  for all  $i \in \mathcal{I}_g$ . Therefore, we have for  $a_s^*$  recommended by Eq. (A.6):

$$\max_{\{a \in \mathcal{A} \mid \exists x \in \mathcal{X}; (a, x) \in \mathcal{B}_n\}} \min_{i \in \mathcal{I}_g} l_n(a, i) - L_x \|x - x(k^*)\| \geq 0.$$

Hence,  $g_i(a_s^*, x(k^*)) \geq 0$  for all  $i \in \mathcal{I}_g$  with probability at least  $1 - \delta$ , which proves the claim.  $\square$

Lemmas A.5 and A.6 show that, if we trigger a backup policy during **GE**, we can guarantee the safety of the experiment before and after switching to the backup policy, respectively.

Next, we prove that, if the backup policy is not triggered during **GE** with parameter  $a_{\mathbf{GE}}$ , then  $a_{\mathbf{GE}}$  is safe with high probability.

**Lemma A.7.** Let the assumptions from Theorem 4.1 and Hypothesis A.1 hold. If, during **GE** with parameter  $a_{\mathbf{GE}}$ , a backup policy is not triggered by our boundary condition, then  $a_{\mathbf{GE}}$  is safe with probability at least  $1 - \delta$ , that is,  $g_i(a_{\mathbf{GE}}, x_0) \geq 0$  for all  $i \in \mathcal{I}_g$ .

*Proof.* Assume the experiment was not safe, i.e., there exists a  $t \geq 0$ , such that for some  $i \in \mathcal{I}_g$   $\bar{g}_i(x(t)) < 0$ . Consider the time step  $k \geq 0$  such that  $t \in [k\Delta t, (k+1)\Delta t]$ . Since, the boundary condition was not triggered during the whole experiment, it was also not triggered at time step  $k$ . This implies that (see Section 4.1.2) there exists a point  $(a_s, x_s) \in \mathcal{B}_n$  such that

$$l_n(a_s, i) - L_x(\|x_s - x(k)\| + \Xi) \geq 0, \quad (\text{A.8})$$

for all  $i \in \mathcal{I}_g$ . Therefore, we have  $g_i(a_s, x(k)) \geq L_x \Xi$  (Hypothesis A.1). Hence, from Lemma A.2 we have  $\bar{g}_i(x(t)) \geq 0$  for all  $i \in \mathcal{I}_g$ . This contradicts our assumption that for some  $t \geq 0$  and  $i \in \mathcal{I}_g$ ,  $\bar{g}_i(x(t)) < 0$ .  $\square$

The following Corollary, summarizes the safety of **GE**.

**Corollary A.8.** Under the assumptions from Theorem 4.1 and Hypothesis A.1 **GoSAFE**OPT is safe during **GE**, i.e., for all  $t \geq 0$ ,  $\bar{g}_i(x(t)) \geq 0$  for all  $i \in \mathcal{I}_g$ .

*Proof.* There are two scenarios that can occur during **GE**.

1. A backup policy is triggered at some time step  $k^* \geq 0$ .
2. The experiment is completed without triggering a backup policy.

For the first case, Lemma A.6 guarantees that we are safe after triggering the backup policy, and Lemma A.5 guarantees that we are safe before we trigger the backup. Combining these two, we obtain that we are safe for scenario 1. For second scenario, Lemma A.7 guarantees safety.  $\square$

We have now shown that under the assumptions of Theorem 4.1 combined with Hypothesis A.1, we can guarantee that we are safe during **GE**, irrespective of whether we trigger a backup policy or not. Particularly, if a backup policy was not triggered, the parameter we experimented with is safe with high probability. We leverage this result to show that Hypothesis A.1 is satisfied for GOSAFE<sub>OPT</sub>.

**Lemma A.9.** Let the assumptions from Theorem 4.1 hold and  $\beta_n$  be defined as in Theorem 3.1. Then, Hypothesis A.1 is satisfied for GOSAFE<sub>OPT</sub>, that is, with probability at least  $1 - \delta$  for all  $i \in \mathcal{I}_g$  and  $n \geq 0$

$$\forall a \in S_n : g_i(a, x_0) \geq 0, \tag{A.9}$$

$$\forall a \in \mathcal{A} : l_n(a, i) \leq g_i(a, x_0) \leq u_n(a, i). \tag{A.10}$$

*Proof.* We use induction on  $n$ .

*Base case  $n = 0$ :* By Assumption 2.1, we have, for all  $a \in S_0$ ,  $g_i(a, x_0) \geq 0$  for all  $i \in \mathcal{I}_g$ . Moreover, the initialization of the confidence intervals presented in Section 3.3 is as follows:  $l_0(a, i) = 0$  if  $a \in S_0$  and  $-\infty$  otherwise, and  $u_0(a, i) = \infty$  for all  $a \in \mathcal{A}$ . Thus, it follows that  $l_0(a, i) \leq g_i(a, x_0) \leq u_0(a, i)$  for all  $a \in \mathcal{A}$ .

*Inductive step:* Our induction hypothesis is  $l_{n-1}(a, i) \leq g_i(a, x_0) \leq u_{n-1}(a, i)$  and  $g_i(a, x_0) \geq 0$  for all  $a \in S_{n-1}$  and for all  $i \in \mathcal{I}_g$ . Based on this, we prove that these relations hold for iteration  $n$ .

We start by showing that  $l_n(a, i) \leq g_i(a, x_0) \leq u_n(a, i)$  for all  $a \in \mathcal{A}$ . To this end, we distinguish between the different updates of the two stages of GOSAFEOP, **LSE** and **GE**. During **LSE**, we define  $l_n(a, i)$  and  $u_n(a, i)$  as

$$\begin{aligned} l_n(a, i) &= \max(l_{n-1}(a, i), \mu_n(a, i) - \beta_n \sigma_n(a, i)), \\ u_n(a, i) &= \min(u_{n-1}(a, i), \mu_n(a, i) + \beta_n \sigma_n(a, i)). \end{aligned}$$

We know that  $g_i(a, x_0) \geq l_{n-1}$  by induction hypothesis and  $g_i(a, x_0) \geq \mu_n(a, i) - \beta_n \sigma_n(a, i)$  with probability  $1 - \delta$  from Theorem 3.1. This implies  $g_i(a, x_0) \geq l_n$ . A similar argument holds for the upper bound.

During **GE**, we update  $l_n(a, i)$  if the parameter we evaluate induces a trajectory that does not trigger a backup policy (see Algorithm 2 line 13). For this parameter, the induction hypothesis allows us to use Lemma A.7 and conclude  $g_i(a, x_0) \geq 0$ . Therefore, the update of the confidence intervals during **GE** also satisfy Eq. (A.10) for iteration  $n$ , thus completing the induction step for the confidence intervals.

As for the confidence intervals, we distinguish between the different updates of the safe set implemented by **LSE** and **GE**. In case of **GE**, we update the safe set by adding the evaluated policy parameter  $a$  only if it does not trigger a backup, i.e.,  $S_n = S_{n-1} \cup \{a\}$ . Following the same argument as above, we can conclude  $g_i(a, x_0) \geq 0$  for all  $i \in \mathcal{I}_g$ . This together with the induction hypothesis means  $g_i(a, x_0) \geq 0$  for all  $i \in \mathcal{I}_g$  and  $a \in S_n$  in case of a **GE** update.

Now we focus on **LSE**. We showed Eq. (A.10) holds for  $n$ . Moreover, we know by induction hypothesis  $g_i(a, x_0) \geq 0$  for all  $a \in S_{n-1}$  and for all  $i \in \mathcal{I}_g$  with high probability. The update equation for the safe set (Eq. (8)) gives for all  $a' \in S_n \setminus S_{n-1}$ , there exists  $a \in S_{n-1}$  such that for all  $i \in \mathcal{I}_g$

$$l_n(a, i) - L_a \|a - a'\| \geq 0. \quad (\text{A.11})$$

We show that this is enough to guarantee with high probability that  $g_i(a', x_0) \geq 0$ . Due to the Lipschitz continuity of the constraint functions, we have

$$\begin{aligned} g_i(a', x_0) &\geq g_i(a, x_0) - L_a \|a - a'\|, \\ &\geq l_n(a, i) - L_a \|a - a'\| \geq 0. \end{aligned} \quad (\text{Eq. (A.11)})$$

Therefore,  $g_i(a', x_0) \geq 0$  for all  $i \in \mathcal{I}_g$  and  $a \in S_n$  with probability at least  $1 - \delta$  also in case of an **LSE** step.

□

Lemma A.9 ensures that Hypothesis A.1 holds for GOSAFE<sub>OPT</sub>. We also

know that under the same assumption as Theorem 4.1 and Hypothesis A.1, we are safe during **GE** (see Corollary A.8). Hence, we can now guarantee safety during **GE**.

Finally, we prove Theorem 4.1, which guarantees safety for GOSAFEOPT.

**Theorem 4.1.** Let Assumptions 2.1 – 2.5 hold and  $\beta_n$  be defined as in Theorem 3.1. Then, GOSAFEOPT guarantees, for all  $n \geq 0$ , that experiments are safe as per Definition 2.6 with probability at least  $1 - \delta$ .

*Proof.* We perform GOSAFEOPT in two stages; **LSE** and **GE**. In Lemma A.9, we proved that for all parameters  $a \in S_n$ ,  $g_i(a, x_0) \geq 0$  for all  $i \in \mathcal{I}_g$  with probability at least  $1 - \delta$ . During **LSE** we query parameters from  $S_n$  (Eq. (9)). Therefore, the experiments are safe. During **GE**, Corollary A.8 proves that when assumptions from Theorem 4.1 and Hypothesis A.1 hold, we are safe during **GE** for our choice of  $\beta_n$ . Furthermore, in Lemma A.9 we proved that Hypothesis A.1 is satisfied for GOSAFEOPT. Hence, we can conclude that if the assumptions from Theorem 4.1 hold, we are safe during **GE** at all times.  $\square$

#### A.2. Optimality Guarantees

In this section, we prove Theorem 4.3 which guarantees that the safe global optimum can be found with  $\epsilon$ -precision if it is discoverable at some iteration  $n \geq 0$  (see Definition 4.2). Then, we show in Lemma A.17 that for many practical applications this discoverability condition is satisfied.

### A.2.1. Proof of Theorem 4.3

We first define the largest region that **LSE** can safely explore for a given safe initialization  $S$  and then we show that we can find the optimum with  $\epsilon$ -precision within this region. To this end, we define the reachability operator  $R_\epsilon^c(S)$  and the fully connected safe region  $\bar{R}_\epsilon^c(S)$  by (adapted from [30; 33])

$$R_\epsilon^c(S) := S \cup \{a \in \mathcal{A} \mid \exists a' \in S \text{ such that } g_i(a', x_0) - \epsilon - L_a \|a - a'\| \geq 0, \\ \forall i \in \mathcal{I}_g\}, \quad (\text{A.12})$$

$$\bar{R}_\epsilon^c(S) := \lim_{n \rightarrow \infty} (R_\epsilon^c)^n(S). \quad (\text{A.13})$$

The reachability operator  $R_\epsilon^c(S)$  contains the parameters we can safely explore if we know our constraint function with  $\epsilon$ -precision within some safe set of parameters  $S$ . Further,  $(R_\epsilon^c)^n(S)$  denotes the repeated composition of  $R_\epsilon^c(S)$  with itself, and  $\bar{R}_\epsilon^c(S)$  its closure. Next, we derive a property for the reachability operator, that we will leverage to provide optimality guarantees.

**Lemma A.10.** Let  $A \subseteq S$ , if  $\bar{R}_\epsilon^c(A) \setminus S \neq \emptyset$ , then  $R_\epsilon^c(S) \setminus S \neq \emptyset$ .

*Proof.* This lemma is a straightforward generalization of [30, Lem. 7.4]. Assume  $R_\epsilon^c(S) \setminus S = \emptyset$ , we want to show that this implies  $\bar{R}_\epsilon^c(A) \setminus S = \emptyset$ . By definition  $R_\epsilon^c(S) \supseteq S$  and therefore  $R_\epsilon^c(S) = S$ . Iteratively applying  $R_\epsilon^c$  to both the sides, we get in the limit  $\bar{R}_\epsilon^c(S) = S$ . Furthermore, because  $A \subseteq S$ , we have  $\bar{R}_\epsilon^c(A) \subseteq \bar{R}_\epsilon^c(S)$  [30, Lem. 7.1]. Thus, we obtain  $\bar{R}_\epsilon^c(A) \subseteq \bar{R}_\epsilon^c(S) = S$ , which leads to  $\bar{R}_\epsilon^c(A) \setminus S = \emptyset$ . □

In the following, we prove that our **LSE** convergence criterion (see Eq. (10))



guarantees that for the safe initialization  $S$ , we can explore  $\bar{R}_\epsilon^c(S)$  during **LSE** in finite time.

**Theorem A.11.** Consider any  $\epsilon > 0$  and  $\delta > 0$ . Let Assumptions 2.2 and 2.3 hold,  $\beta_n$  be defined as in Theorem 3.1, and  $S \subseteq \mathcal{A}$  be an initial safe seed of parameters, i.e.,  $g(a, x_0) \geq 0$  for all  $a \in S$ . Assume that the information gain  $\gamma_n$  grows sublinearly with  $n$  for the kernel  $k$ . Further let  $n^*$  be the smallest integer such that (cdf. the convergence criterion of **LSE** in Eq. (10))

$$\max_{a \in \mathcal{G}_{n^*-1} \cup \mathcal{M}_{n^*-1}} \max_{i \in \mathcal{I}} w_{n^*-1}(a, i) < \epsilon \text{ and } S_{n^*-1} = S_{n^*}. \quad (\text{A.14})$$

Then we have that  $n^*$  is finite and when running **LSE**, the following holds with probability at least  $1 - \delta$  for all  $n \geq n^*$ :

$$\bar{R}_\epsilon^c(S) \subseteq S_n, \quad (\text{A.15})$$

$$f(\hat{a}_n) \geq \max_{a \in \bar{R}_\epsilon^c(S)} f(a) - \epsilon, \quad (\text{A.16})$$

with  $\hat{a}_n = \arg \max_{a \in S_n} l_n(a, 0)$ .

*Proof.* We first leverage the result from [30, Thm. 4.1] which provides the following *worst-case* bound on  $n^*$

$$\frac{n^*}{\beta_{n^*} \gamma_{|\mathcal{I}|n^*}} \geq \frac{C_1 (\bar{R}_0^c(S)) + 1}{\epsilon^2}, \quad (\text{A.17})$$

where  $C_1 = 8/\log(1 + \sigma^{-2})$  and  $n^*$  is the smallest integer that satisfies Eq. (A.17). Hence, we have that  $n^*$  is finite. The sublinear growth of  $\gamma_n$  with  $n$  is satisfied for many practical kernels, like the ones we consider in this work [43].

Next, we prove Eq. (A.15). For the sake of contradiction, assume  $\bar{R}_\epsilon^c(S) \setminus S_{n^*} \neq \emptyset$ . This implies,  $R_\epsilon^c(S_{n^*}) \setminus S_{n^*} \neq \emptyset$  (Lemma A.10). Therefore, there exists some  $a \in \mathcal{A} \setminus S_{n^*}$  such that for some  $a' \in S_{n^*} = S_{n^*-1}$  (Eq. (A.14)), we have for all  $i \in \mathcal{I}_g$

$$\begin{aligned} 0 &\leq g_i(a', x_0) - \epsilon - L_a \|a - a'\|, \\ &\leq u_{n^*-1}(a', i) - L_a \|a - a'\|. \end{aligned} \quad (\text{Lemma A.9})$$

Therefore,  $a' \in \mathcal{G}_{n^*-1}$  (see [30] or Appendix C Definition C.1) and accordingly,  $w_{n^*-1}(a', i) < \epsilon$ . Next, because  $w_{n^*-1}(a', i) < \epsilon$ , we have for all  $i \in \mathcal{I}_g$

$$0 \leq g_i(a', x_0) - \epsilon - L_a \|a - a'\| \leq l_{n^*-1}(a', i) - L_a \|a - a'\|. \quad (\text{A.18})$$

This means  $a \in S_{n^*}$  (Eq. (8)), which is a contradiction. Thus, we conclude that  $\bar{R}_\epsilon^c(S) \subseteq S_{n^*}$  and because  $S_{n^*} \subseteq S_n$  for all  $n \geq n^*$  (Proposition A.12), we get  $\bar{R}_\epsilon^c(S) \subseteq S_n$ .

Now we prove Eq. (A.16). Consider any  $n \geq n^*$ . Note,  $w_{n^*-1}(a', i) < \epsilon$ , implies  $w_n(a', i) < \epsilon$  (see Algorithm 1 line 4 or Algorithm 2 line 13). For simplicity, we denote the solution of  $\arg \max_{a \in \bar{R}_\epsilon^c(S)} f(a)$  as  $a_S^*$ . We have

$$\begin{aligned} u_n(a_S^*, 0) &\geq f(a_S^*) && (\text{Lemma A.9}) \\ &\geq f(\hat{a}_n) && (\text{by definition of } a_S^*) \\ &\geq l_n(\hat{a}_n, 0) && (\text{Lemma A.9}) \\ &= \max_{a \in S_n} l_n(a, 0). && (\text{by definition of } \hat{a}_n) \end{aligned}$$

Therefore,  $a_S^*$  is a maximizer, i.e.,  $a_S^* \in \mathcal{M}_n$  (see Appendix C Definition C.2) and has uncertainty less than  $\epsilon$ , that is,  $w_n(a_S^*, i) < \epsilon$ . Now, we show that  $f(\hat{a}_n) \geq f(a_S^*) - \epsilon$ . For the sake of contradiction assume,

$$f(\hat{a}_n) < f(a_S^*) - \epsilon. \quad (\text{A.19})$$

Then we obtain,

$$\begin{aligned} l_n(a_S^*, 0) &\leq l_n(\hat{a}_n, 0) && (\text{by definition of } \hat{a}_n) \\ &\leq f(\hat{a}_n) && (\text{Lemma A.9}) \\ &< f(a_S^*) - \epsilon && (\text{by Eq. (A.19)}) \\ &\leq u_n(a_S^*, 0) - \epsilon && (\text{Lemma A.9}) \\ &\leq u_n(a_S^*, 0) - w_n(a_S^*, 0) && (\text{because } w_n(a_S^*, 0) \leq \epsilon) \\ &= l_n(a_S^*, 0), && (\text{by definition of } w_n(a_S^*, 0)) \end{aligned}$$

which is a contradiction. Therefore, we have  $f(\hat{a}_n) \geq f(a_S^*) - \epsilon$ .

□

Theorem A.11 states that for a given safe seed  $S$ , the convergence of **LSE** (Eq. (10)) implies that we have discovered its fully connected safe region  $\bar{R}_\epsilon^c(S)$  and recovered the optimum within the region with  $\epsilon$ -precision.

Based on the previous results, we can show that if the safe global optimum is discoverable for some iteration  $n \geq 0$  (see Definition 4.2), then we can find an approximately optimal safe solution. However, to prove optimality, what we also require is that if  $a^* \in S_n$  then  $a^* \in S_{n+1}$ . Otherwise, we might have the global optimum in our safe set for some iteration  $n$  but we may lose it

for some  $n_1 > n$ . GOSAFEOPT guarantees that  $S_n \subseteq S_{n+1}$  and therefore this cannot happen.

**Proposition A.12.** Let the assumptions from Theorem 4.1 hold. For any  $n \geq 0$ , the following property is satisfied for  $S_n$ .

$$S_n \subseteq S_{n+1}, \tag{A.20}$$

*Proof.* The safe set provably increases during **LSE** [30, Lem. 7.1]. During **GE**, the safe set is only updated if a new safe parameter is found. The proposed update also has the non-decreasing property (see Algorithm 2, line 13). Hence, we can conclude that  $S_n \subseteq S_{n+1}$ .  $\square$

Proposition A.12 shows that if the safe global optimum  $a^* \in S_n$ , then  $a^* \in S_{n+1}$ . Next, we prove that if a new safe region  $A$  is added to our safe set  $S_n$ , we will explore its largest reachable safe set  $\bar{R}_\epsilon^c(A)$ .

**Lemma A.13.** Consider any integer  $n \geq 0$ . Let  $S_n$  be the safe set of parameters explored after  $n$  iterations of GOSAFEOPT and let  $\beta_n$  be defined as in Theorem 3.1. Consider  $A = S_{n+1} \setminus S_n$ . If  $A \neq \emptyset$ , then there exists a finite integer  $\bar{n} > n$  such that  $\bar{R}_\epsilon^c(A) \cup \bar{R}_\epsilon^c(S_n) \subseteq S_{\bar{n}}$  with probability at least  $1 - \delta$ .

*Proof.* First, if  $\bar{R}_\epsilon^c(A) \setminus S_{\bar{n}} = \emptyset$  and  $\bar{R}_\epsilon^c(S_n) \setminus S_{\bar{n}} = \emptyset$  then  $\bar{R}_\epsilon^c(A) \cup \bar{R}_\epsilon^c(S_n) \subseteq S_{\bar{n}}$ . We now show that  $\bar{R}_\epsilon^c(A) \setminus S_{\bar{n}} = \emptyset$ . Assume that  $\bar{R}_\epsilon^c(A) \setminus S_{\bar{n}} \neq \emptyset$ . We know that  $A \subseteq S_{n+1} \subseteq S_{\bar{n}}$  (Proposition A.12). This implies  $R_\epsilon^c(S_{\bar{n}}) \setminus S_{\bar{n}} \neq \emptyset$  (Lemma A.10). Since  $A \neq \emptyset$ , the safe set is expanding. For GOSAFEOPT, this can either happen during **LSE** or during **GE** when a new parameter is

successfully evaluated, i.e., the boundary condition is not triggered. In either case, we perform **LSE** till convergence. Let  $\bar{n} > n$  be the smallest integer for which we converge during **LSE**, i.e., for which

$$\max_{a \in \mathcal{G}_{\bar{n}-1} \cup \mathcal{M}_{\bar{n}-1}} \max_{i \in \mathcal{I}} w_{\bar{n}-1}(a, i) < \epsilon \text{ and } S_{\bar{n}-1} = S_{\bar{n}} \quad (\text{A.21})$$

holds. From Theorem A.11, we know that  $\bar{n}$  is finite. Consider  $a \in R_c^\epsilon(S_{\bar{n}}) \setminus S_{\bar{n}}$ . Then we have that there exists  $a' \in S_{\bar{n}}$  such that  $0 \leq g_i(a', x_0) - \epsilon - L_a \|a - a'\|$  (see Eq. (A.12)). Furthermore,  $S_{\bar{n}-1} = S_{\bar{n}}$ , means  $a' \in S_{\bar{n}-1}$ . Hence, we also have  $0 \leq u_{\bar{n}-1}(a, i) - L_a \|a - a'\|$ , which implies that,  $a' \in \mathcal{G}_{\bar{n}-1}$  (Appendix C Definition C.1) and therefore,  $w_{\bar{n}-1}(a', i) < \epsilon$ . This implies that  $0 \leq l_{\bar{n}-1}(a', i) - L_a \|a - a'\|$ . Therefore, according to Eq. (8),  $a \in S_{\bar{n}}$ , which is a contradiction. Hence,  $\bar{R}_c^\epsilon(A) \setminus S_{\bar{n}} = \emptyset$ . We can proceed similarly to show that  $\bar{R}_c^\epsilon(S_n) \setminus S_{\bar{n}} = \emptyset$ . Since we have  $\bar{R}_c^\epsilon(A) \setminus S_{\bar{n}} = \emptyset$  and  $\bar{R}_c^\epsilon(S_n) \setminus S_{\bar{n}} = \emptyset$ , we can conclude that  $\bar{R}_c^\epsilon(A) \cup \bar{R}_c^\epsilon(S_n) \subseteq S_{\bar{n}}$ .  $\square$

In Lemma A.13 we have shown that for every set  $A$  that we add to our safe set, we will explore its fully connected safe region in finite time. This is crucial because it allows us to guarantee that when we discover a new region during **GE**, we explore it till convergence. Finally, we can now prove Theorem 4.3.

**Theorem 4.3.** Let  $a^*$  be a safe global optimum. Further, let Assumptions 2.1 – 2.5 hold,  $\beta_n$  be defined as in Theorem 3.1. Assume there exists a finite integer  $\tilde{n} \geq 0$  such that  $a^*$  is discoverable at iteration  $\tilde{n}$  (see Definition 4.2). Then, there exists a finite integer  $n^* \geq \tilde{n}$  such that with probability at least  $1 - \delta$ ,

$$f(\hat{a}_n) \geq f(a^*) - \epsilon, \quad \forall n \geq n^* \quad (13)$$

with  $\hat{a}_n = \arg \max_{a \in S_n} l_n(a, 0)$ .

*Proof.* Since,  $a^*$  is discoverable at iteration  $\tilde{n}$ , there exists a set  $A^* \subseteq S_{\tilde{n}}$  such that  $a^* \in \bar{R}_\epsilon^c(A^*)$ . Furthermore, we have  $\bar{R}_\epsilon^c(A^*) \subseteq \bar{R}_\epsilon^c(S_{\tilde{n}})$  (Lemma A.13), therefore,  $a^* \in \bar{R}_\epsilon^c(S_{\tilde{n}})$ . Additionally, in GOSAFEOP, we explore each safe region till we have uncertainty less than  $\epsilon$  in the maximizer and expander set (see Eq. (10)). Theorem A.11 shows that we can find the optimum in the safe region with  $\epsilon$  precision in finite time  $n^* \geq \tilde{n}$ . Hence, there exists a finite integer  $n^*$  such that

$$f(\hat{a}_n) \geq f(a^*) - \epsilon, \quad \forall n \geq n^*. \quad (\text{A.22})$$

with  $\hat{a}_n = \arg \max_{a \in S_n} l_n(a, 0)$ .

□

#### A.2.2. Requirements for Discovering Safe Sets with **GE**

In the previous section, we showed that if a safe global optimum  $a^*$  is discoverable at some iteration  $\tilde{n}$ , we can then find it with  $\epsilon$ -precision. In this section, we show that if for a parameter  $a_{\mathbf{GE}}$  in  $\mathcal{A} \setminus S_n$ , we have backup policies for all the states in its trajectory, then  $a_{\mathbf{GE}}$  will be eventually added to our safe set of parameters. Finally, we conclude this section by showing that for many practical cases,  $a^*$  fulfills the discoverability condition.

Now, we derive conditions that allow us to explore new regions/parameters during **GE**. To this end, we start by defining a set of safe states  $\mathcal{X}_n^s$ , i.e., the states for which our boundary condition does not trigger a backup policy (cf. Fig. A.10).

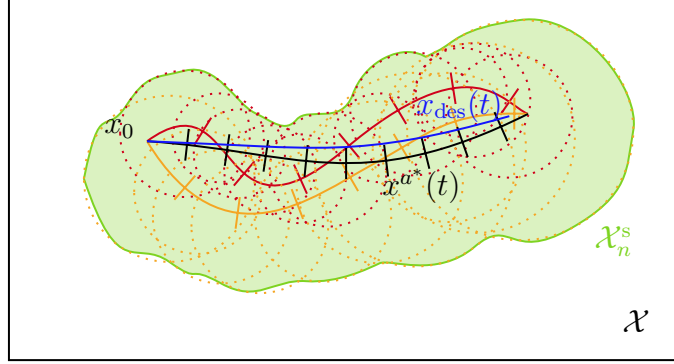


Figure A.10: Illustration of  $\mathcal{X}_n^s$ . In orange and red are safe trajectories starting at  $x_0$ , in blue the desired trajectory, and in black the trajectory of the safe global optimum. For each state we visit during a safe experiment with parameter  $a$ , we determine a ball of states for which  $a$  can be used as a backup parameter. The union of these balls is  $\mathcal{X}_n^s$ . Since for many practical tasks safe policies visit similar set of states, knowing backup policies for states in  $\mathcal{X}_n^s$  is sufficient to find the global optimum.

**Definition A.14.** The set of safe states  $\mathcal{X}_n^s$  is defined as

$$\mathcal{X}_n^s := \bigcup_{(a', x') \in \mathcal{B}_n} \left\{ x \in \mathcal{X} \mid \|x' - x\| \leq \frac{1}{L_x} \min_{i \in \mathcal{I}_g} l_n(a', i) - \Xi, \right\}. \quad (\text{A.23})$$

Intuitively, if a trajectory induced by a parameter being evaluated during **GE** lies in  $\mathcal{X}_n^s$ , then the boundary condition will not be triggered for this parameter. As a result, it will be discovered by **GoSAFE**OPT. Now we will prove that this set of safe states  $\mathcal{X}_n^s$  is non-decreasing. This is an important property because it tells us that **GoSAFE**OPT continues to learn backup policies for more and more states.

**Lemma A.15.** Let the assumptions from Theorem 4.1 hold. For any  $n \geq 0$ , the following property is satisfied for  $\mathcal{X}_n^s$ .

$$\mathcal{X}_n^s \subseteq \mathcal{X}_{n+1}^s. \quad (\text{A.24})$$

*Proof.* The lower bounds  $l_n(a, i)$  are non-decreasing for all  $i \in \mathcal{I}$  by definition (see Algorithm 1 line 4 or Algorithm 2 line 13). Additionally, because we continue to add new rollouts to our set of backups, we have  $\mathcal{B}_n \subseteq \mathcal{B}_{n+1}$  (see Algorithm 1 line 3 or Algorithm 2 line 12). For each  $x \in \mathcal{X}_n^s$ , there exists  $(a_s, x_s) \in \mathcal{B}_n$ , such that  $l_n(a_s, i) - L_x(\|x - x_s\| + \Xi) \geq 0$  for all  $i \in \mathcal{I}_g$ . Because  $\mathcal{B}_n \subseteq \mathcal{B}_{n+1}$  and  $l_{n+1}(a_s, i) \geq l_n(a_s, i)$ ,  $x \in \mathcal{X}_{n+1}^s$ .  $\square$

Next, we state conditions under which a parameter  $a_{\mathbf{GE}} \in \mathcal{A} \setminus S_n$  will be discovered during **GE**, i.e., no backup policy would be triggered during **GE**, in finite time.

**Lemma A.16.** Consider any  $n \geq 0$ . Let  $S_n$  be the safe set of parameters explored after  $n$  iterations of GOSAFE<sub>OPT</sub> and  $a_{\mathbf{GE}}$  a parameter in  $\mathcal{A} \setminus S_n$ . Further, let the assumptions from Theorem 4.3 hold and  $\beta_n$  be defined as in Theorem 3.1. If, for all  $k \geq 0$ ,  $x^{a_{\mathbf{GE}}}(k) \in \mathcal{X}_n^s$ , where,  $x^{a_{\mathbf{GE}}}(k)$  represents the state at time step  $k$  for the system starting at  $x_0$  with policy  $\pi^{a_{\mathbf{GE}}}(\cdot)$ , then there exists a finite integer  $\tilde{n} > n$ , such that  $a_{\mathbf{GE}} \in S_{\tilde{n}}$ .

*Proof.* Assume that there exists no finite integer  $\tilde{n} > n$  such that  $a_{\mathbf{GE}} \in S_{\tilde{n}}$ . This would imply that  $a_{\mathbf{GE}} \in \mathcal{A} \setminus S_{\tilde{n}}$  for all  $\tilde{n} > n$ . Thus, because  $a_{\mathbf{GE}}$  will never be a part of our safe set, it will never be evaluated during **LSE**. However, from Theorem A.11 we know that **LSE** will converge in finite number of iterations after which we will perform **GE**. Since  $a_{\mathbf{GE}}$  is not a part of the safe set, it can only be evaluated during **GE**, where parameters outside of the safe regions are queried. The parameter space  $\mathcal{A}$  is finite and any parameter that was evaluated unsuccessfully, i.e., boundary condition was triggered, will be added to  $\mathcal{E}$  and therefore not evaluated again (see Eq. (11))



and Algorithm 2 line 9). This implies that  $a_{\mathbf{GE}}$  will be evaluated for some  $n'$  with  $n < n' < \tilde{n}$  (since  $S_{n'} \subseteq S_{\tilde{n}}$ , see Proposition A.12). Furthermore,  $\mathcal{X}_n^s \subseteq \mathcal{X}_{n'}^s$  (Lemma A.15) and, therefore, for all  $k \geq 0$ ,  $x^{a_{\mathbf{GE}}}(k) \in \mathcal{X}_{n'}^s$ . If when  $a_{\mathbf{GE}}$  is evaluated, the experiment is unsuccessful, i.e., we were to trigger a backup policy, this would imply that for some  $k'$  and  $i \in \mathcal{I}_g$ , there is no  $(a_s, x_s) \in \mathcal{B}_{n'}$  such that

$$l_{n'}(a, i) \geq L_x(\|x^{a_{\mathbf{GE}}}(k') - x_s\| + \Xi).$$

Thus, we had  $x^{a_{\mathbf{GE}}}(k') \notin \mathcal{X}_{n'}^s$ , which contradicts our assumption. Therefore,  $a_{\mathbf{GE}} \in S_{n'+1} \subseteq S_{\tilde{n}}$  (Proposition A.12), which is a contradiction. Consequently, we have  $a_{\mathbf{GE}} \in S_{\tilde{n}}$  after a finite number of iterations  $\tilde{n}$ .  $\square$

Lemma A.16 guarantees that, if the trajectory of parameter  $a_{\mathbf{GE}}$  lies in  $\mathcal{X}_n^s$ , then it will eventually be added to our safe set, either during **LSE** or during **GE**. We utilize this result to provide a condition for the safe global optimum  $a^*$  to be *discoverable* at iteration  $\tilde{n}$  by GOSAFE<sub>OPT</sub>.

**Lemma A.17.** Consider any  $n \geq 0$ . Let Assumptions 2.1 – 2.4 hold,  $\beta_n$  be defined as in Theorem 3.1, and let  $a^* \in \mathcal{A}$  be the safe global optimum. If there exists  $a_{\mathbf{GE}} \in \mathcal{A} \setminus S_n$  such that

- (i) for all  $k \geq 0$ ,  $x^{a_{\mathbf{GE}}}(k) \in \mathcal{X}_n^s$ , where  $x^{a_{\mathbf{GE}}}(k)$  is the state visited by the system starting at  $x_0$  under the policy  $\pi^{a_{\mathbf{GE}}}(\cdot)$  at time step  $k$ , and
- (ii)  $a^* \in \bar{R}_\epsilon^c(\{a_{\mathbf{GE}}\})$ ,

then  $a^*$  is discoverable at iteration  $\tilde{n} \geq n$  by GOSAFE<sub>OPT</sub> with probability at least  $1 - \delta$ .

*Proof.* Since, for all  $k \geq 0$ ,  $x^{a_{\mathbf{GE}}}(k) \in \mathcal{X}_n^s$ , there exists a finite integer  $\tilde{n} > n$  such that  $a_{\mathbf{GE}} \in S_{\tilde{n}}$  (Lemma A.16). Furthermore, because  $a^* \in \bar{R}_\epsilon^c(\{a_{\mathbf{GE}}\})$ , we can conclude that  $a^*$  is discoverable at iteration  $\tilde{n}$  (see Definition 4.2).  $\square$

The condition here is interesting because empirically, for many practical cases, it is fulfilled. Crucially, optimal or near-optimal parameters tend to visit similar states as other safe policies. We add rollouts from safe policies to our set of backups  $\mathcal{B}_n$  and therefore have backup policies for their trajectories and other trajectories that lie close to them. Therefore, the trajectories of (near-)optimal parameters lie in  $\mathcal{X}_n^s$  (see Fig. A.10) and in this case the safe global optimum fulfills the discoverability condition from Theorem 4.3. Thus, for many practical cases, GoSAFEOPt can find the safe global optimum with  $\epsilon$ -precision.

## B. Additional Information on Experiments

For all our experiments in Section 5, we consider a controller in the operational space. The operational space dynamics of the end-effector are given by [47]

$$u(x(t)) = \Lambda(q)\ddot{s} + \Gamma(q, \dot{q})\dot{s} + \eta(q), \quad (\text{B.1})$$

where  $s$  represents the end-effector position,  $q$  the joint angles, and  $\Lambda(q)$ ,  $\Gamma(q, \dot{q})$ ,  $\eta(q)$  are nonlinearities representing the mass, Coriolis, and gravity terms, respectively. The state we consider is  $x(t) = [s^T(t), \dot{s}^T(t)]^T$

We apply an impedance controller:

$$u(x(t)) = -K \begin{bmatrix} s \\ \dot{s} \end{bmatrix} + \Gamma(q, \dot{q})\dot{s} + \eta(q), \quad (\text{B.2})$$

with  $K$  being the feedback gain. The torque  $\tau$  applied to each of the joints can be calculated via  $\tau = J^T u(x(t))$ , with  $J$  the Jacobian.

Furthermore, the constraints we consider for our experiments are of the form stated in Assumption 2.5. For our experiments, we can directly measure  $g(a, x(k))$ , where  $k$  denotes discrete time step. Therefore, instead of using  $l_n(a_s, i)$  for the boundary condition in Section 4.4.2, we take a lower bound over all the tuples in our set of backups,  $\mathcal{B}_n$ , i.e.,  $l_n(a_s, x_s, i)$ , which could potentially reduce the conservatism of the boundary condition. However, to determine  $l_n(a_s, x_s, i)$ , we require a GP which is defined over the parameter and state space, and contains all the points from  $\mathcal{B}_n$ . The set  $\mathcal{B}_n$  consists of rollouts from individual experiments, as we mention later we typically add 50–100 data points from each experiment to  $\mathcal{B}_n$ . Therefore, after conducting 10 experiments, our GP has around 1000 datapoints. This makes doing inference costly. To this end, we use a subset selection scheme to select a small subset of points  $(a, x)$  from  $\mathcal{B}_n$  at random with a probability that is proportional to  $\exp(-\min_{i \in \mathcal{I}_g} l_n^2(a, x, i))$ . Crucially, we want to retain points that have a small lower bound such that we have low uncertainty around these points. We perform this subset selection once our GP has acquired more than  $n_{\max}$  data points. Then, we select a subset of  $m < n_{\max}$  points.

Lastly, for the boundary condition from Section 4.4.2, we can define the distance  $d_u$  and  $d_l$  through the covariance function of our GP. Specifically, for stationary isotropic kernels, we can define the distances  $d_u$  (same for  $d_l$ ) such that  $\|x - x'\| \leq d_u \implies k(\|x - x'\|) \geq \kappa_u^2$ . This makes the choice of  $d_u$  more intuitive since it directly relates to the covariance function of our GP.

### B.1. Simulation

For the simulation task, we determine the impedance  $K$  using an infinite horizon LQR parameterized via

$$Q = \begin{bmatrix} Q_r & 0 \\ 0 & \kappa_d Q_r \end{bmatrix}, Q_r = 10^{q_c} I_3,$$

$$R = 10^{r-2} I_3, A = \begin{bmatrix} 0 & I_3 \\ 0 & 0 \end{bmatrix}, B = \begin{bmatrix} 0 \\ I_3 \end{bmatrix}.$$

The matrices  $A$ ,  $B$  are obtained assuming that we use a feedback linearization controller [47]. However, because we instead use an impedance controller, there are nonlinearities and imprecisions in our model. The parameters  $q_c, r, \kappa_d$  are tuning parameters we would like to optimize.

The control input we apply is:

$$u(x(t)) = -K \begin{bmatrix} s - s_{\text{des},L}(k) \\ \dot{s} \end{bmatrix} + \Gamma(q, \dot{q})\dot{s} + \eta(q),$$

where  $s_{\text{des},L}(k)$  is a discretized target position defined as

$$s_{\text{des},L}(k) = s_0 + \frac{k}{T_{\text{traj}}}(s_{\text{des}} - s_0).$$

Thus, we linearly increase our target, the speed of which is proportional to  $\frac{1}{T_{\text{traj}}}$ . The constraint and stage rewards (i.e., rewards received at each time

step [1]) are:

$$\begin{aligned}
\bar{g}(x(t)) &= \frac{\|s(t) - s_{\text{des}}\|_2 - \|s(0) - s_{\text{des}}\|_2}{\|s(0) - s_{\text{des}}\|_2} - \alpha, \quad \alpha = 0.08 \\
\mathcal{R}(x(t)) &= -\|s(t) - s_{\text{des}}\|_2^2 / \|s(0) - s_{\text{des}}\|_2^2 \\
&\quad - \frac{1}{25} \|\tanh \dot{s}(t)\|_2^2 - \frac{1}{25} \|\tanh u(x(t))\|_2^2.
\end{aligned} \tag{B.3}$$

Hence, the objective encourages reaching the target as fast as possible. But, penalizes large velocities and actions. Furthermore, we want to limit the overshoot in the end-effector’s position. Additionally, to encourage fast behaviour, we only sample parameters for which the eigenvalues of  $A - BK$  are less than a fixed threshold:  $\text{eig}(A - BK) \leq -10$ . Although this constraint is independent of the state, it can be evaluated before each experiment and parameters can be rejected if the criterion is not fulfilled. As states, we consider the end-effector position relative to  $s_{\text{des}}$  and velocity. The parameters we optimize over are  $q_c, r$ . The value for  $\kappa_d$  is heuristically set to 0.1 based on our observations of the simulation.

We observe that the underlying functions  $f, g_i$  exhibit non-smooth behaviour. Therefore we use the Matérn kernel [42] with parameter  $\nu = 3/2$  for our GP. Furthermore, we pick a horizon of  $T = 2000$  steps only collect the states visited during the initial 500 time steps. Given that the horizon is considerably larger than 500, we consider these initial states to be safe if the experiment was safe. Additionally, even though we collect the initial 500 states, a lot of them in general would lie close-by. Hence, we sample 50 out of 500 collected data uniformly at random and add them to our GP. Therefore, per experiment, we collect 50 data points.

We restrict our parameter search space to a normalized domain  $q_n \times r_n \in [1/3, 1] \times [-1, 1]$  with  $q_c = 6q_n$  and  $r = 3r_n$ .

We initialize SAFEOPt with a policy in the lower half of the safe set (see Fig. 7), i.e.,  $S_0 = \{(5, -2.7), (4, -3), (6, -2)\}$ . Furthermore, we normalize the objective and the constraint values and therefore pick  $\kappa_i = 1$  for the kernel. We proceed similarly for GOSAFEOPt.

### B.2. Hardware

For the hardware task we apply the following controller:

$$u(x(t)) = -K \begin{bmatrix} s(t) - s_{\text{des}}(t) \\ \dot{x} \end{bmatrix} + \Gamma(q, \dot{q})\dot{s} + \eta(q). \quad (\text{B.4})$$

Furthermore, we define the subsequent objective and constraint functions:

$$\begin{aligned} \mathcal{R}(x(t)) &= -\|s(t) - s_{\text{des}}(t)\|_2, \\ \bar{g}(s(t)) &= \|s(t) - s_w\|_{P,\infty} - \psi, \end{aligned}$$

where  $s_w$  represents the center of the wall in Fig. 6 and  $\|s - s_w\|_{P,\infty} \leq d_w$  defines the rectangular shaped outline around the wall and  $\psi > d_w$ .

For the task, we use a squared exponential (SE) kernel [42]. Additionally, due to the symmetric nature of the trajectory, we consider all the states visited during an experiment to be safe. In particular, by choosing the last state of our trajectory to be a terminal state, we can assume the problem has an infinite horizon. Lastly, we sample 100 points at random from the collected rollout and add them to our respective GPs.

## C. Additional Definitions

In this section, we present some of the definitions from SAFE<sub>OPT</sub> and GoSAFE for completeness.

**Definition C.1.** The expanders  $\mathcal{G}_n$  are defined as  $\mathcal{G}_n := \{a \in S_n \mid e_n(a) > 0\}$  with  $e_n(a) = |\{a' \in \mathcal{A} \setminus S_n, \exists i \in \mathcal{I}_g : u_n(a, i) - L_a \|a - a'\| \geq 0\}|$ .

**Definition C.2.** The maximizers  $\mathcal{M}_n$  are defined as  $\mathcal{M}_n := \{a \in S_n \mid u_n(a, 0) \geq \max_{a' \in S_n} l_n(a', 0)\}$ .

**Definition C.3.** GoSAFE's discretized state space is defined as  $\mathcal{X}_\mu$ :  $\forall x \in \mathcal{X}, \exists [x]_\mu \in \mathcal{X}_\mu$  with  $\|x - [x]_\mu\|_1 \leq \mu$ , where  $[x]_\mu$  is the state in  $\mathcal{X}_\mu$  closest to  $x$  in the  $\ell_1$ -norm.

**Definition C.4.** The safe set  $S_n$  in the joint parameter and state space is defined as

$$S_n := S_{n-1} \cup \left( \bigcap_{i \in \mathcal{I}_g} \bigcup_{(a, \tilde{x}_0) \in S_{n-1}} \{(a', \tilde{x}'_0) \in \mathcal{A} \times \mathcal{X}_\mu \mid l_n(a, \tilde{x}_0, i) - L_a \|a - a'\|_1 - L_x(\|\tilde{x}_0 - \tilde{x}'_0\|_1 + \mu) \geq 0\} \right). \quad (\text{C.1})$$

## D. Hyperparameters

The hyperparameters of our simulated and real-world experiments are provided in Tables D.2 and D.3.

Table D.2: Hyperparameters of the simulation task

	SAFEOPT	GoSAFEOPT
Iterations	200	200
$\beta_n^{1/2}$	4	4
$a$ lengthscale	0.12,0.12	0.12,0.12
$\kappa$ for $f$ and $g$	1, 1	1, 1
$\sigma$ for $f$ and $g$	0.1,0.1	0.1,0.1
$x$ lengthscale	-	0.3,0.3,0.3, 2.5,2.5,2.5
$\epsilon$	-	0.1
max <b>LSE</b> steps	-	30
max <b>GE</b> steps	-	10
$\kappa_l$	-	0.90
$\kappa_u$	-	0.94
$\eta_l$	-	0.4
$\eta_u$	-	0.6
$n_{\max}$	-	1000
$m$	-	500



Table D.3: Hyperparameters of hardware task

	SAFEOPTSWARM	GoSAFEOPT
Iterations	50	50
$\beta_n^{1/2}$	3	3
$a$ lengthscale	0.1,0.1,0.1	0.1,0.1,0.1
$\kappa$ for $f$ and $g$	1, 1	1, 1
$\sigma$ for $f$ and $g$	0.05,0.3	0.05,0.3
$x$ lengthscale	-	0.3,0.3,0.2, 0.5,0.5,0.3
$\epsilon$	-	0.01
max <b>LSE</b> steps	-	20
max <b>GE</b> steps	-	5
$\kappa_l$	-	0.90
$\kappa_u$	-	0.94
$\eta_l$	-	0.9
$\eta_u$	-	1.1
$n_{\max}$	-	1000
$m$	-	500